

RESEARCH ARTICLE

IBR5 Modulates Temperature-Dependent, R Protein CHS3-Mediated Defense Responses in *Arabidopsis*

Jingyan Liu¹✉, Haibian Yang¹✉, Fei Bao¹, Kevin Ao², Xiaoyan Zhang¹, Yuelin Zhang², Shuhua Yang²*

1 State Key Laboratory of Plant Physiology and Biochemistry, College of Biological Sciences, National Plant Gene Research Center, China Agricultural University, Beijing, China, **2** Department of Botany, University of British Columbia, Vancouver, British Columbia, Canada

✉ These authors contributed equally to this work.

* yangshuhua@cau.edu.cn.



 OPEN ACCESS

Citation: Liu J, Yang H, Bao F, Ao K, Zhang X, Zhang Y, et al. (2015) IBR5 Modulates Temperature-Dependent, R Protein CHS3-Mediated Defense Responses in *Arabidopsis*. *PLoS Genet* 11(10): e1005584. doi:10.1371/journal.pgen.1005584

Editor: Gitta Coaker, University of California Davis, UNITED STATES

Received: February 23, 2015

Accepted: September 16, 2015

Published: October 9, 2015

Copyright: © 2015 Liu et al. This is an open access article distributed under the terms of the [Creative Commons Attribution License](https://creativecommons.org/licenses/by/4.0/), which permits unrestricted use, distribution, and reproduction in any medium, provided the original author and source are credited.

Data Availability Statement: All relevant data are within the paper and its Supporting Information files.

Funding: This work was supported by the National Key Scientific Research Project (2015CB910203), the National Natural Science Foundation of China (31330006 and 31228003) and the China National Funds for Distinguished Young Scientists (31225003) to SY. The funders had no role in study design, data collection and analysis, decision to publish, or preparation of the manuscript.

Competing Interests: The authors have declared that no competing interests exist.

Abstract

Plant responses to low temperature are tightly associated with defense responses. We previously characterized the chilling-sensitive mutant *chs3-1* resulting from the activation of the Toll and interleukin 1 receptor-nucleotide binding-leucine-rich repeat (TIR-NB-LRR)-type resistance (R) protein harboring a C-terminal LIM (Lin-11, Isl-1 and Mec-3 domains) domain. Here we report the identification of a suppressor of *chs3*, *ibr5-7* (*indole-3-butyric acid response 5*), which largely suppresses chilling-activated defense responses. *IBR5* encodes a putative dual-specificity protein phosphatase. The accumulation of CHS3 protein at chilling temperatures is inhibited by the *IBR5* mutation. Moreover, *chs3*-conferred defense phenotypes were synergistically suppressed by mutations in *HSP90* and *IBR5*. Further analysis showed that *IBR5*, with holdase activity, physically associates with CHS3, HSP90 and SGT1b (Suppressor of the G2 allele of *skp1*) to form a complex that protects CHS3. In addition to the positive role of *IBR5* in regulating CHS3, *IBR5* is also involved in defense responses mediated by R genes, including *SNC1* (*Suppressor of npr1-1, Constitutive 1*), *RPS4* (*Resistance to P. syringae 4*) and *RPM1* (*Resistance to Pseudomonas syringae pv. maculicola 1*). Thus, the results of the present study reveal a role for *IBR5* in the regulation of multiple R protein-mediated defense responses.

Author Summary

Resistance (R) genes play central roles in recognizing pathogens and triggering plant defense responses. *CHS3* encodes a TIR-NB-LRR-type R protein harboring a C-terminal LIM domain. A point mutation in *CHS3* activates the defense response under chilling stress. Here we identified and characterized *ibr5-7*, a mutant that suppresses the chilling-induced defense responses of *chs3-1*. We observed that the enhanced defense responses and cell death in the *chs3-1* mutant are synergistically dependent on *IBR5* and *HSP90*. *IBR5* physically interacts with *CHS3*, forming a complex with SGT1b/ HSP90. Moreover,

IBR5 is also involved in the R-gene resistance mediated by *SNC1*, *RPS4* and *RPM1*. Thus, IBR5 plays key roles in regulating defense responses mediated by multiple R proteins.

Introduction

Plant growth and development are continuously affected by various environmental stresses, including low temperature and pathogen infection. Emerging evidence has shown that the defense responses of plants are regulated by temperatures [1]. Temperature modulates the defense responses induced by certain types of resistance (R)/R-like proteins, including Toll/Interleukin-1 receptor (TIR)-nucleotide-binding (NB)-leucine-rich repeat (LRR) proteins [N (Resistance to tobacco mosaic virus) in tobacco; RPP1 (Recognition of *Peronospora parasitica* 1)-like, RPP4, RPS4 (Resistance to *P. syringae* 4) and SNC1 (Suppressor of *npr1-1*, Constitutive 1) in *Arabidopsis*], CC-NB-LRR proteins [Rx in tomato; RPM1 (Resistance to *Pseudomonas syringae* *pv.* *maculicola* 1) and RPS2 in *Arabidopsis*], LRR-TM (transmembrane-domain) proteins (Cf-4 and Cf-9 in tomato), TM-CC proteins [RPW8 (Resistance to Powdery Mildew 8) in *Arabidopsis*] [2–7], and the TIR-NB protein CHS1 (chilling sensitive 1) in *Arabidopsis* [8]. A recent study showed that low temperatures (10°C to 23°C) elevate R protein-mediated effector-triggered immunity (ETI), and higher temperatures (23°C to 32°C) lead to a shift in pattern-triggered immunity (PTI) signaling in plants [9]. These studies suggest that temperature largely affects the function of R proteins.

Recent studies have revealed that a number of components regulate the activities of R proteins, which in turn finely tune defense signaling. Chaperone and co-chaperone proteins, such as the HSP90-SGT1b (Suppressor of the G2 allele of *skp1*)-RAR1 (Required for MLA12 resistance 1) complex, involve in multiple R protein-mediated defense pathways [10]. Earlier reports have indicated that these complexes are required for the correct folding and/or stability of R proteins [11–13]. However, several recent studies have suggested that both SGT1b and HSP90 play positive roles in the degradation of R proteins, including RPM1, RPS2 and SNC1, by the SCF complex [14–16]. The dual functions of R protein regulators ensure that the plant immunity system rapidly and properly responds to pathogen invasion. In addition to these chaperones, many other regulators are also involved in R protein regulation. A series of regulators of SNC1 were identified by screening suppressors and enhancers of *snc1-1*, have been shown to regulate the chromatin, transcription and protein levels of SNC1. These proteins include E1 and E4 ligases, U-box proteins, acetyltransferases, RNA binding proteins, nuclear pore complex components [13,17–22]. These results suggest that SNC1 and/or other R proteins are regulated by multiple biological processes including nucleo-cytoplasmic trafficking, transcriptional reprogramming, RNA processing and protein modification.

Previous studies have shown that low temperature activates defense responses in plants harboring mutations in R/R-like genes, including *CHS1*, *CHS2/RPP4* and *CHS3* [7,8,23]. *Arabidopsis* *CHS3* encodes a TIR-NB-LRR-type R protein harboring a C-terminal LIM domain [23,24]. The *chs3-1* mutant exhibits chilling-sensitive phenotypes, including small stature and increased disease resistance. The SGT1b and RAR1 proteins are required for R protein stability [25–27]. The *chs3* chilling-sensitive phenotypes are suppressed in *sgt1b* and *rar1* mutants [23]. However, the molecular regulatory mechanism of the temperature-dependent defense responses through *CHS3* remains elusive.

In the present study, we identified *ibr5-7* as a suppressor of the chilling-sensitive phenotypes of *chs3-1*. *IBR5* (*Indole-3-Butyric Acid Response 5*) encodes a dual-specificity MAPK phosphatase, which acts as a positive regulator of plant responses to auxin and ABA [28]. *IBR5*

physically interacts with MPK12, and activated MPK12 is dephosphorylated and inactivated by IBR5, thereby negatively regulating auxin signaling [29]. Here, we observed that *ibr5* suppresses the chilling-sensitive phenotypes of *chs3-1* independently of MPK12. Biochemical data showed that IBR5 complexes with CHS3 and HSP90-SGT1b to stabilize CHS3. Moreover, IBR5 is involved in the *R*-gene mediated resistance specified by *SNC1*, *RPS4* and *RPM1*. Thus, IBR5 plays an important role in regulating different R protein-mediated defense responses.

Results

Identification of the suppressor of *chs3-1*, *suc5*

The *chs3-1* plants are dwarfed and have small, curly leaves. The defense responses in *chs3-1* are constitutively active at 16°C, but this phenotype is alleviated at higher temperatures (22°C) [23]. To understand the molecular mechanism underlying the temperature-dependent cell death in the *chs3-1* mutant, we performed a genetic screen to identify suppressors of *chs3-1* (*suc*). The *chs3-1* seeds were mutagenized with ethyl methylsulfonate (EMS), and the M2 population was screened for mutants with wild-type morphology at 16°C. Among the suppressors screened, most of the variations were second-site, loss-of-function mutations in *CHS3*, thereby rescuing the *chs3* chilling-sensitive phenotype. One suppressor harbored a mutation in *RAR1*, and two suppressors harbored mutations in *SGT1b*; these genes are important regulators required for *CHS3* function [23]. These results indicate that the genetic screen was effective. Here, we characterized *suc5* as a new suppressor of *chs3-1*. The *chs3 suc5* mutant plants largely resembled wild-type plants when grown at 16°C, except these plants exhibited a slightly smaller stature compared with the wild type and had serrated true leaves (Fig 1A).

suc5 suppresses cell death and defense responses of *chs3-1* upon chilling stress

Previous studies have indicated that extensive cell death and strong defense responses occur in *chs3-1* mutants grown at 16°C [23]. To determine whether the *suc5* mutation affects these cell death-related phenotypes, *chs3-1* plants were grown at 16°C, followed by staining with trypan blue and 3, 3'-diaminobenzidine (DAB). The *suc5* mutation dramatically reduced the extensive cell death observed in *chs3-1* mutants grown at 16°C (Fig 1B). Furthermore, the accumulation of hydrogen peroxide (H₂O₂) in *chs3 suc5* plants grown at 16°C was dramatically reduced compared with *chs3-1* (Fig 1C).

The *chs3-1* mutant also accumulates high levels of salicylic acid (SA) [23]. To determine whether *suc5* inhibits SA accumulation in *chs3-1* at 16°C, the endogenous SA level in *chs3 suc5* plants was measured. Both the free and total SA levels were dramatically reduced in *chs3 suc5* plants grown at 16°C compared with the *chs3* mutant (Fig 1D). Because *PR* genes were highly expressed in *chs3-1*, we further examined the expression of the *PR* genes in *chs3 suc5* plants grown at 16°C. Quantitative real-time PCR (qRT-PCR) analysis showed that the expression of *PR1*, *PR2* and *CHS3* was significantly reduced in *chs3 suc5* plants grown at 16°C (Fig 1E and 1F).

Compared with wild-type plants, *chs3-1* plants grown at 16°C exhibit enhanced resistance to a virulent pathogenic strain of *Pseudomonas syringae* pv tomato (*P.s.t.*), DC3000 [23]. To investigate the role of *SUC5* in the *chs3*-mediated basal defense response, the response of *chs3 suc5* seedlings to *P.s.t.* DC3000 was analyzed. The *suc5* mutation fully suppressed the *chs3*-conferred constitutive resistance to *P.s.t.* DC3000, resulting in wild-type-like susceptibility (Fig 1G). Taken together, these results demonstrated that, under chilling stress, the *suc5* mutation largely suppresses all known autoimmune phenotypes of *chs3*.

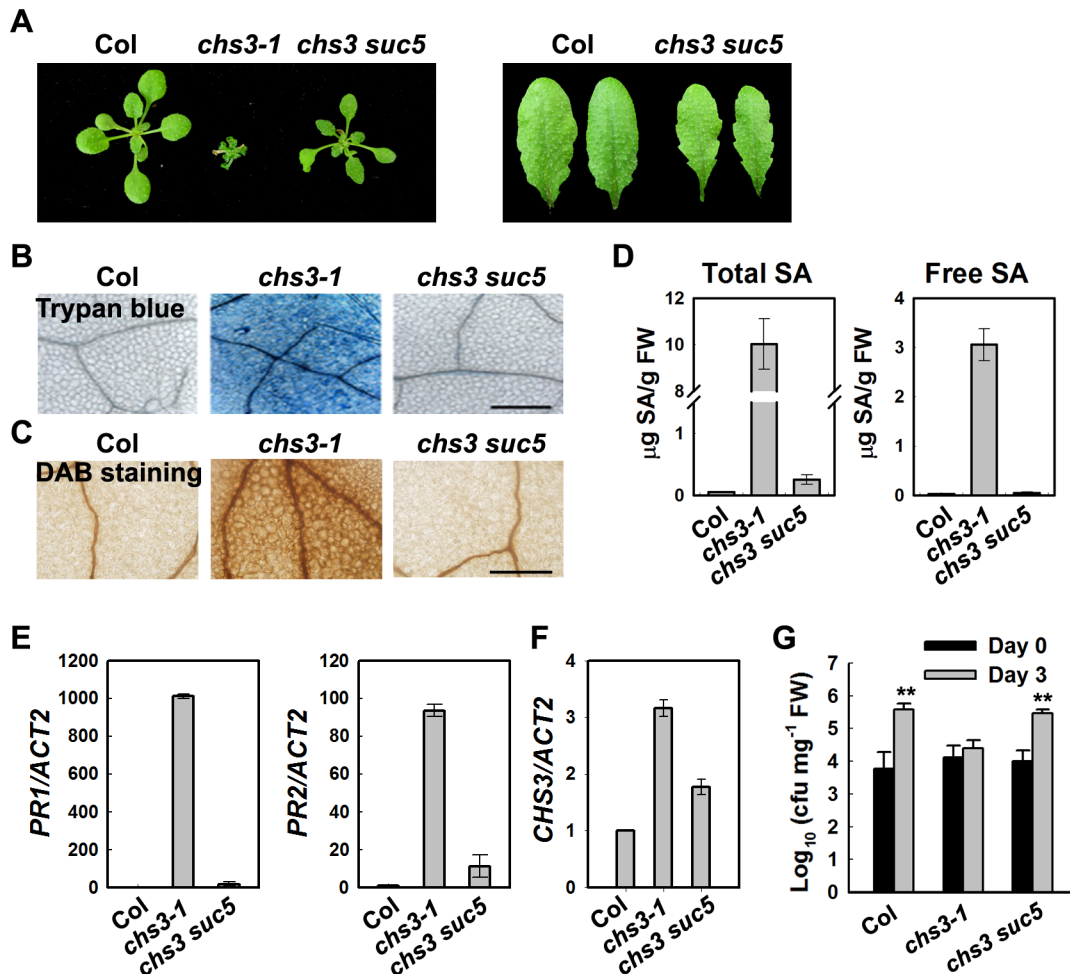


Fig 1. Identification of a suppressor of *chs3-1*, *suc5*. (A) Morphology of wild-type (Col), *chs3-1* and *chs3 suc5* plants grown at 16°C. The photographs show 4-week-old plants grown in soil (left panel). The rosette leaves of *chs3 suc5* have increased leaf serration compared with Col (right panel). (B, C) Trypan blue and DAB staining of leaves from 3-week-old wild type, *chs3-1* and *chs3 suc5* plants grown at 16°C. Bars: 200 μm . (D) Levels of total and free SA in 4-week-old, wild-type, *chs3-1* and *chs3 suc5* plants grown at 16°C. (E, F) Expression of *PR1*, *PR2* (E) and *CHS3* (F) genes in 3-week-old wild-type, *chs3-1* and *chs3 suc5* plants grown at 16°C. The values were normalized to the expression of *ACTIN2*. The error bars represent the SD of three replicates. Similar results were obtained in three independent experiments. (G) Growth of *P.s.t.* DC3000 on wild-type, *chs3-1*, and *chs3 suc5* plants. Three-week-old plants were dipped with *P.s.t.* DC3000 ($\text{OD}_{600} = 0.05$). Bacterial growth was monitored as described in the Materials and Methods. The error bars represent the SD of three replicates, and the asterisks indicate significant differences compared with wild-type Col (** $P < 0.01$, *t*-test).

doi:10.1371/journal.pgen.1005584.g001

The *SUC5* gene is *IBR5*

To map the *suc5* mutation, *chs3 suc5* in Columbia (Col) was crossed with Landsberg *erecta* (*Ler*) to generate a mapping population. Among the F2 progeny, 50 plants homozygous or heterozygous at the *chs3-1* locus and exhibiting a wild-type morphology at 16°C were used for rough mapping. The *suc5* mutation was initially mapped to the top of chromosome II (Fig 2A). Fine mapping using approximately 200 plants refined the mutation to a 500-kb region between markers F3C11 and F5G3 (Fig 2A). Further sequencing analysis of this region in *chs3 suc5* revealed a G-to-A substitution in the first exon of *At2g04550*, resulting in an amino substitution from Arg to Lys (Fig 2A).

At2g04550 was previously identified as *IBA RESPONSE5* (*IBR5*), which encodes a putative dual-specificity protein phosphatase [28]. To determine whether the mutation in *IBR5* is responsible for the suppression the phenotypes of *chs3*, a *chs3 ibr5-3* double mutant was

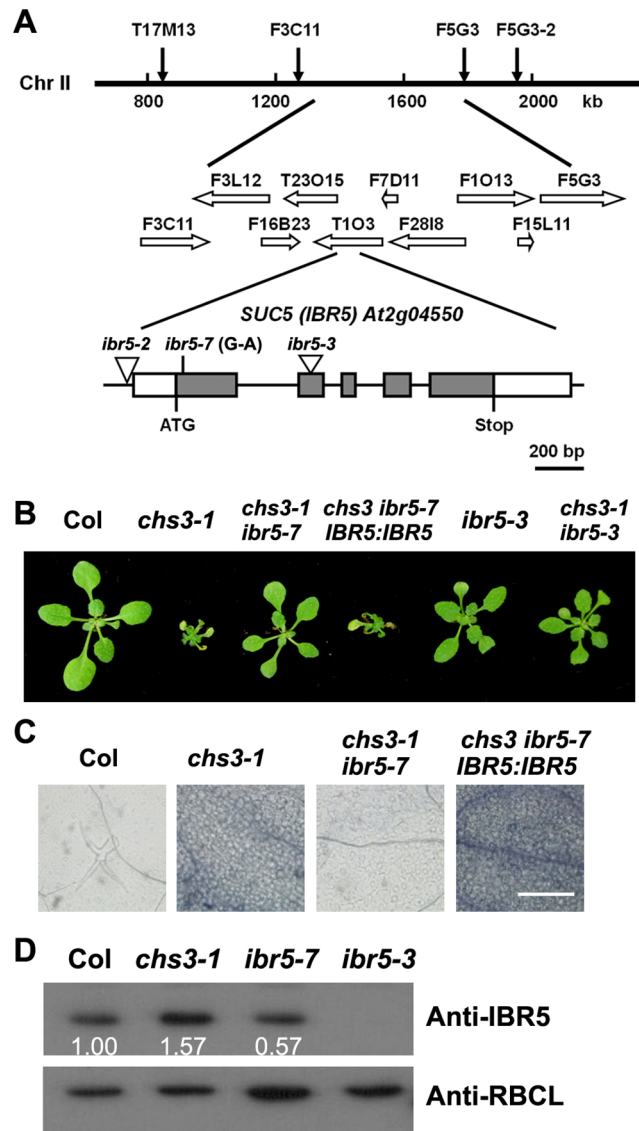


Fig 2. Identification of *SUC5*. (A) Map position and genomic structure of the *SUC5* gene. Exons, introns and UTRs are presented as gray boxes, lines and white boxes, respectively. The point mutation and T-DNA insertions are shown. (B) Morphology of the wild-type, *chs3-1*, *chs3-1 ibr5-7*, complemented transgenic plants (*IBR5:IBR5 chs3 ibr5-7*), T-DNA insertion mutant (*ibr5-3*) and *chs3-1 ibr5-3* double mutant. The photographs show 3-week-old plants grown in soil at 16°C. (C) Trypan blue staining of true leaves from wild-type, *chs3-1*, *chs3-1 ibr5-7* and *IBR5:IBR5 chs3-1 ibr5-7* plants. Bars: 200 µm. (D) IBR5 protein levels in wild-type, *chs3-1* and *ibr5* mutants. Total protein was extracted from 2-week-old seedlings. IBR5 protein was analyzed by immunoblotting using an anti-IBR5 antibody. Anti-RBCL was used as a loading control.

doi:10.1371/journal.pgen.1005584.g002

generated by crossing *chs3-1* with *ibr5-3* [29]. The *ibr5-3* mutant largely restored the growth defects of *chs3-1* mutant plants grown at 16°C (Fig 2B). Furthermore, a wild-type genomic *IBR5* fragment containing 5.0 kb of the 5'-promoter region and the 3' untranslated region was transformed into the *chs3 suc5* mutant. All eight T1 transgenic plants displayed *chs3*-conferred morphological and cell death phenotypes (Fig 2B and 2C). Taken together, these results indicate that *SUC5* is indeed *IBR5*. Therefore, *suc5* was renamed *ibr5-7*.

The *ibr5-7* single mutant was isolated by crossing *chs3 ibr5-7* with wild-type Col plants. Immunoblot analysis showed that the IBR5 protein level in *ibr5-7* was lower than that in the

wild-type Col plants, whereas no IBR5 protein was detected in *ibr5-3* (Fig 2D). Intriguingly, IBR5 protein accumulated in the *chs3-1* mutant (Fig 2D), implying that IBR5 might stabilize CHS3 protein. Consistent with a previous study on *ibr5* loss-of-function mutants [28], *ibr5-7* displayed serrated leaves and was resistant to high concentrations of exogenous auxins, including IAA, IBA and 2, 4-D (S1 Fig). These results indicate that *ibr5-7* is a novel null allele of *IBR5*.

IBR5 interacts with CHS3

To further investigate whether IBR5 physically interacts with CHS3 in CHS3-mediated signaling, a yeast two-hybrid assay was performed. As a TIR-NB-LRR-LIM-containing protein, the full-length CHS3 protein is approximately 185 kD and is difficult to express in yeast. Therefore, truncated constructs individually carrying the TIR, NB, LRR, unknown and LIM domains of CHS3 were generated and transformed into yeast (Fig 3A). IBR5 directly interacted with the TIR domain of CHS3 in yeast (Fig 3B).

Previous studies have shown that CHS3 localizes to the nucleus [24], consistent with the results of the present study (S2B Fig). We also observed that IBR5 localized to both the cytosol and the nucleus (S2A and S2B Fig). To determine whether CHS3 interacts with IBR5 *in vivo*, 35S:HA-Flag-IBR5 (HF-IBR5) and the Myc-tagged TIR domain of CHS3 driven by the Super promoter (*TIR-Myc*) were transiently expressed in *Arabidopsis* mesophyll protoplasts, and subsequently, a co-immunoprecipitation (co-IP) assay was performed. IBR5 precipitated the TIR domain of CHS3 (Fig 3C). Moreover, HF-IBR5 interacted with full-length CHS3-1-Myc (the mutated form of CHS3 containing the same mutation as the *chs3-1* mutant) when expressed in *N. benthamiana* (Fig 3D). These results indicated that CHS3 interacts with IBR5 through the TIR domain of CHS3 *in vivo*.

IBR5 belongs to a family of dual specificity protein phosphatases (DSPs), and the conserved cysteine in the conserved motif (VxVHCx2GxSRx5AYLM) of DSPs is necessary for catalytic activity in many DSP proteins, including IBR5 and its homolog DsPTP1 [30]. To examine whether the phosphatase activity of IBR5 is required for interactions with CHS3, we generated the mutated form of IBR5 (IBR5^{C129S}). The yeast two-hybrid assay showed that the mutation did not affect the interaction of IBR5 and CHS3 (Fig 3B), suggesting that the catalytic activity is not necessary for the interaction between IBR5 and CHS3. We next introduced *Super:IBR5--Myc* and *Super:IBR5^{C129S}-Myc* into the *chs3 ibr5* mutant background (Fig 3E, 3F and 3G). As a control, *IBR5-Myc* fully recovered the *chs3 ibr5* phenotype and *PR1* expression. However, the morphological phenotypes and *PR1* expression of *chs3 ibr5* were partially rescued in the mutated *IBR5^{C129S}-Myc* plants (Fig 3F and 3G). These results suggest that the catalytic activity of IBR5 is required for full function in the CHS3-mediated defense response.

IBR5 promotes CHS3 accumulation at both transcription and protein levels

Another gain-of-function *chs3* mutant, *chs3-2D*, was dwarfed and exhibited a constitutively active defense phenotype at 22°C [24]. Moreover, *chs3:chs3-2D-GFP* transgenic plants were generated, exhibiting *chs3-2D*-like phenotypes [24]. To examine whether *IBR5* affects the accumulation of CHS3 in *chs3-2D-GFP* plants, *ibr5-3 chs3-2D-GFP* plants were generated by crossing *ibr5-3* with *chs3-2D-GFP* plants (Fig 4A). The dwarf phenotype of *chs3-2D-GFP* plants was fully restored by *ibr5-3* (Fig 4B), and GFP signals were observed in the nuclei of *chs3-2D-GFP* transgenic plants (Fig 4C). However, no obvious GFP signal was detectable in *ibr5-3 chs3-2D-GFP* plants (Fig 4C). Consistently, the expression of *PR* genes in *chs3-2D-GFP* was also suppressed in *ibr5-3* plants (Fig 4D). The expression of *CHS3* in *ibr5-3 chs3-2D-GFP* plants was also examined. As shown in Fig 4E, *CHS3* expression in *ibr5-3 chs3-2D-GFP* plants was

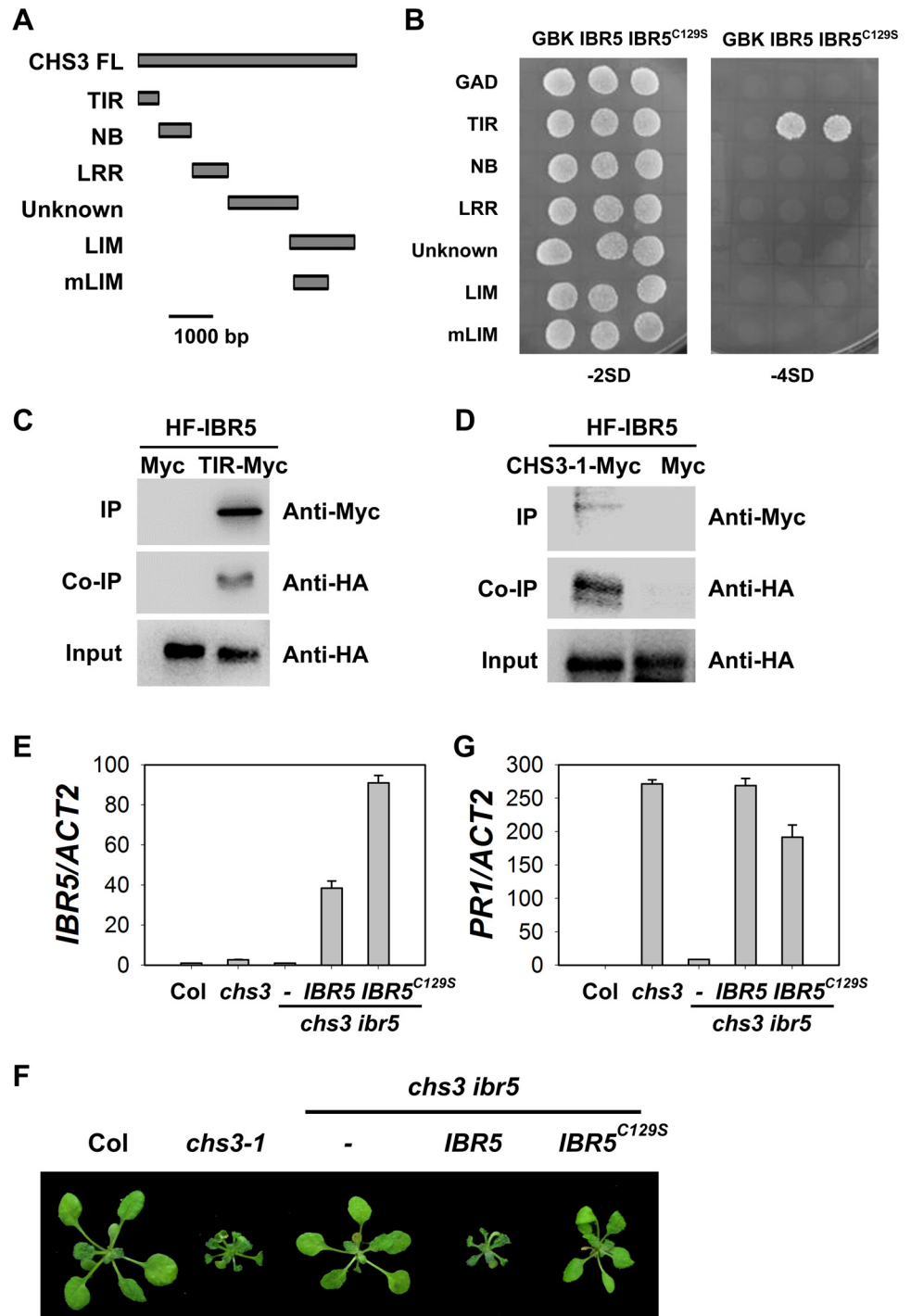


Fig 3. Interaction of IBR5 with CHS3. (A) Predicted protein structure of CHS3. TIR, Toll/Interleukin-1 receptor domain (aa 1–138); NB, nucleotide binding domain (aa 139–468); LRR, leucine-rich repeat domain (aa 469–729); Unknown, domain with no known function (aa 730–1240); LIM, LIM (Lin-11, Isl-1 and Mec-3 domains)-containing domain (aa 1135–1614); mLIM, LIM-containing domain with the same mutation in *chs3-1*, which contains a stop codon at 1422. (B) Interaction between IBR5 and CHS3 in yeast. The different CHS3 domains shown in (A) were fused with the pGADT7 vector. IBR5 and mutated IBR5^{C129S} were fused with the pGBKT7 vector. The constructs were transformed into AH109 yeast cells and spotted onto SD media lacking Trp and Leu (-2SD) or lacking Trp, Leu, His and Ade (-4SD). The experiments were performed four times with similar results. (C) Co-immunoprecipitation of IBR5 and the TIR domain of CHS3. Total proteins were extracted from protoplasts expressing 35S:HA-Flag-IBR5 (35S:HF-IBR5) with Super: TIR domain of CHS3

(*Super:TIR-Myc*) or *Super:Myc*, and immunoprecipated with anti-Myc antibody. The proteins were obtained from crude lysates (Input) and the immunoprecipated proteins were detected using an anti-HA antibody. (D) Interaction of IBR5 and full-length CHS3 *in vivo*. Total proteins were extracted from *N. benthamiana* leaves transfected with 35S:*HF-IBR5* and *Super:CHS3-1-Myc*, and were immunoprecipated with anti-Myc antibody. The proteins from crude lysates (Input) and the immunoprecipated proteins were detected using an anti-HA antibody. (E) Expression of *IBR5* in 3-week-old *Super:IBR5-Myc* and *Super:IBR5^{C129S}-Myc* transgenic plants in *chs3 ibr5* grown at 16°C. (F) The phenotypes of *Super:IBR5-Myc* and *Super:IBR5^{C129S}-Myc* transgenic plants in *chs3 ibr5*. The photographs show 3-week-old plants grown in soil at 16°C. (G) The expression of *PR1* in 3-week-old *Super:IBR5-Myc* and *Super:IBR5^{C129S}-Myc* transgenic *chs3 ibr5* plants grown at 16°C.

doi:10.1371/journal.pgen.1005584.g003

dramatically decreased compared with *chs3-2D-GFP* plants, consistent with the result obtained in *chs3 ibr5-7* (Fig 1F). Moreover, the expression of *CHS3* was down-regulated in the *ibr5-3* mutant (Fig 4F). These results suggest that IBR5 positively regulates the expression of *CHS3*, which might at least be partially responsible for the decreased *CHS3-2D-GFP* signals in *ibr5-3 chs3-2D-GFP*.

To dissect the influence of IBR5 on *CHS3* at the protein level, we examined the effect of IBR5 on the *CHS3* protein level in *Arabidopsis* protoplasts. The protein level of *CHS3-1-Myc* in protoplasts co-expressing *CHS3-1-Myc* and *HF-IBR5* was much higher than that in protoplasts expressing *CHS3-1-Myc* and *HF* (Fig 4G). This result suggests that IBR5 also promotes the accumulation of *CHS3* protein in plant.

HSP90 and IBR5 synergistically regulate *chs3*-conferred phenotypes

HSP90 plays an important role in the stability of R proteins [31]. A previous study showed that the *hsp90.3-1* mutant was a suppressor of the *chs2/rpp4-1d* mutant [32]. Therefore, we examined whether *hsp90.3-1* rescues the chilling-sensitive phenotype of *chs3-1*. The *chs3-1 hsp90.3-1* double mutant was generated and largely showed wild-type morphology but was smaller at 16°C (Fig 5A), and cell death was dramatically suppressed (Fig 5B). *PR1* expression was also significantly inhibited in the double mutant (Fig 5C). Further analysis showed that the F1 progeny of *ibr5 chs3* and *hsp90.3 chs3* could partially rescue the morphology, cell death and *PR1* gene expression of *chs3* (Fig 5A, 5B and 5C). Moreover, the *chs3 hsp90.3 ibr5* triple mutant more closely resembled wild-type plants than the *chs3 hsp90* and *chs3 ibr5* mutants in terms of growth, cell death and *PR1* gene expression (Fig 5A, 5B and 5C). These data indicate that HSP90 and IBR5 synergistically modulate the *chs3*-conferred growth and defense responses.

IBR5 interacts with HSP90 and SGT1b

HSP90 functions as a complex with SGT1b and RAR1 [11,33–35] and we previously showed that *sgt1b* and *rar1* suppressed the phenotypes of *chs3-1* [23], similar to *ibr5* (Fig 1). Next we determined whether IBR5 physically interacts with HSP90 and SGT1b in plants. To this end, a luciferase complementation imaging (LCI) assay was performed in *Nicotiana benthamiana*. IBR5 interacted with HSP90 and SGT1b in *N. benthamiana* leaves (Fig 6A and 6B). Furthermore, co-IP assays showed that endogenous HSP90 successfully immunoprecipitated IBR5-Myc in transgenic plants expressing *IBR5-Myc*, but not in *Myc* transgenic plants (Fig 6C). Similarly, SGT1b could be co-immunoprecipitated with IBR5 in transgenic plants expressing *IBR5-Myc* and *SGT1b-FLAG*, but not in transgenic plants expressing *Myc* and *SGT1b-FLAG* (Fig 6D). We also examined the association between SGT1b and *CHS3*. Co-IP assays showed that SGT1b associated with the TIR domain of *CHS3* and full-length *CHS3-1 in vivo* (S3 Fig). Furthermore, we examined the interaction of *CHS3-1* with IBR5 and SGT1b in *N. benthamiana* leaves. As shown in Fig 6E, *CHS3-1* could simultaneously pull down IBR5 and SGT1b in plants. These results indicate that IBR5 forms complex(es) with *CHS3*, HSP90 and SGT1b *in vivo*.

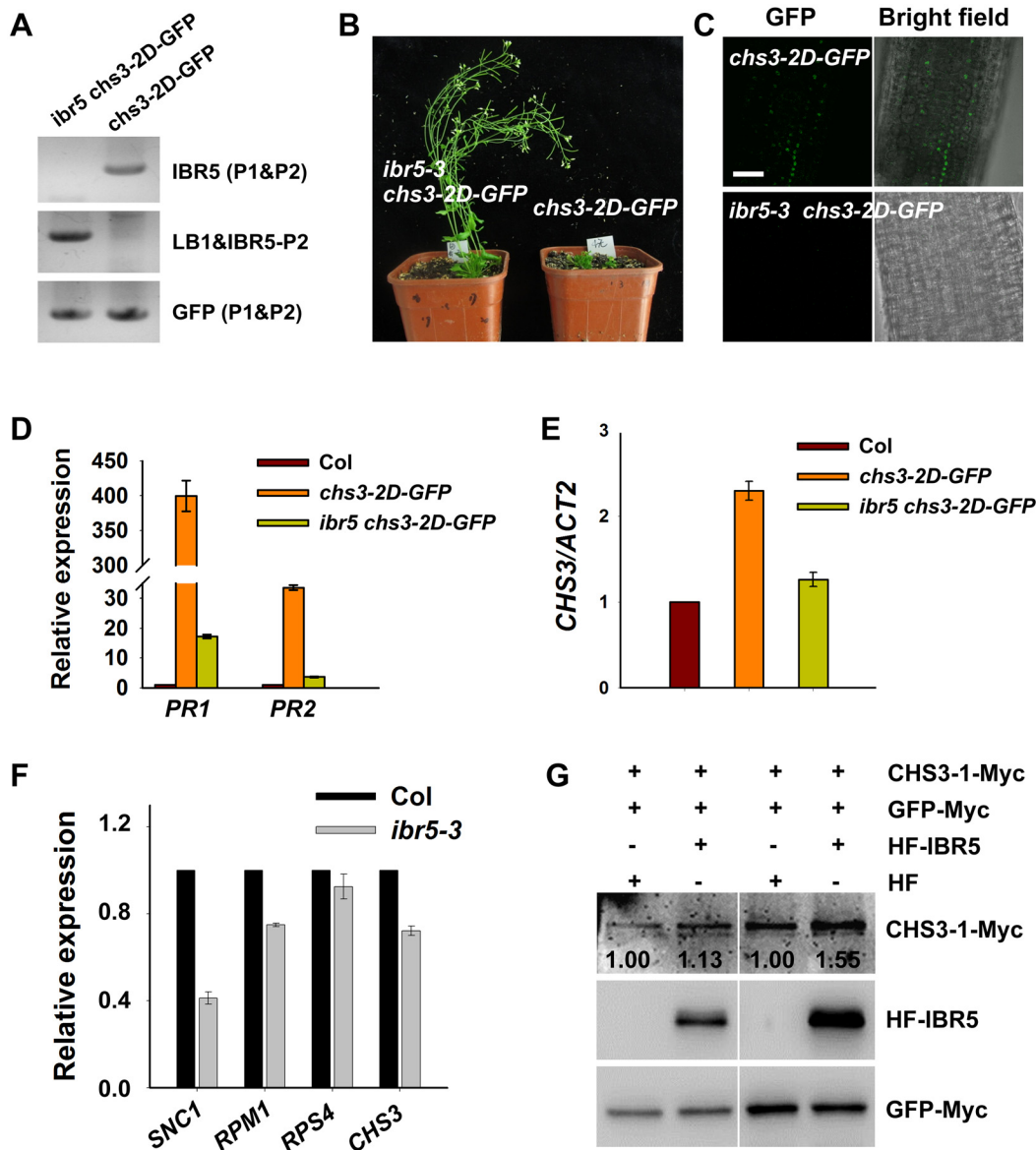


Fig 4. CHS3 is promoted by IBR5 at both mRNA and protein levels. Genotyping of *ibr5-3 chs3-2D-GFP* plants. The primers used for genotyping the *chs3-2D-GFP* gene were GFP-P1 and GFP-P2, and the primers used for genotyping *ibr5-3* were IBR5-P1, IBR5-P2 and LB1 as listed in S1 Table. The phenotype of *chs3-2D-GFP* transgenic plants was rescued by *ibr5-3*. *chs3-2D-GFP* and *ibr5-3 chs3-2D-GFP* plants were grown for 5 weeks, and representative plants are shown. Expression of CHS3-2D-GFP protein in 8-d-old *chs3-2D-GFP* and *ibr5-3 chs3-2D-GFP* plants. Bar: 100 μ m. (D) Expression of CHS3-2D-GFP protein in 8-day-old *chs3-2D-GFP* and *ibr5-3 chs3-2D-GFP* plants. Bar: 100 μ m. (D, E) Expression of the *PR1*, *PR2* (D) and *CHS3* (E) genes in *chs3-2D-GFP* and *ibr5-3 chs3-2D-GFP* plants. The values were normalized to the expression of *ACTIN2*. The error bars represent the SD of three replicates. (F) The expression of several *R* genes (*SNC1*, *RPM1*, *RPS4* and *CHS3*) in 10-day-old *ibr5-3* mutant grown at 22°C. The values were normalized to the expression of *ACTIN2*. The error bars represent the SD of three replicates. Similar results were obtained in three independent experiments. (G) The effect of IBR5 on the CHS3 protein level in *Arabidopsis* protoplasts. *Super:CHS3-1-Myc* and *35S:HF-IBR5* or *35S:HF* constructs were co-expressed in *Arabidopsis* protoplasts. IBR5 and CHS3 proteins were detected using anti-HA and anti-Myc antibodies. The *GFP-Myc* construct was used as a control for transformation efficiency. The numbers show the ratios of CHS3-1-Myc to GFP-Myc protein levels. Two biological repeats are shown with similar results.

doi:10.1371/journal.pgen.1005584.g004

IBR5 exhibits holdase activity *in vitro*

We subsequently investigated whether IBR5 protects proteins *in vitro* using a thermal aggregation assay with citrate synthase (CS) as a model substrate [36]. CS aggregation was examined after measuring the absorbance at 500 nm under thermally denaturing conditions (40°C or

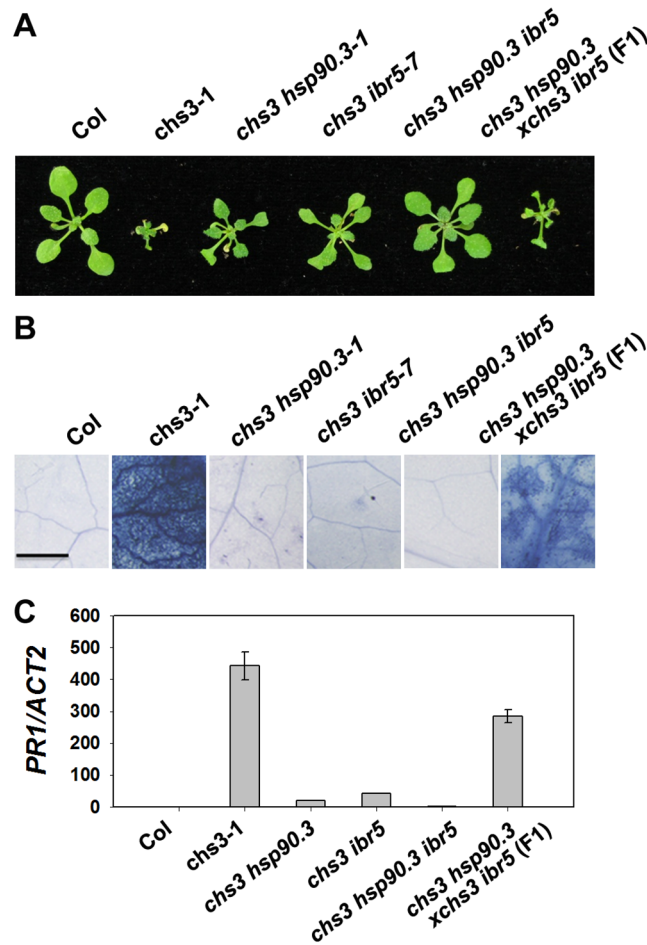


Fig 5. Genetic analysis of CHS3, IBR5 and HSP90.3. (A) Morphology of 4-week-old wild-type Col, *chs3-1*, *chs3 hsp90.3-1*, *chs3 ibr5-7*, *chs3 hsp90.3 ibr5* and F1 progeny of *chs3 hsp90.3-1* crossed with *chs3 ibr5-7* grown in soil at 16°C. (B) Trypan blue staining of the leaves from the plants described in (A). Bar: 50 μm. (C) *PR1* gene expression in the plants described in (A). The values were normalized to the expression of *ACTIN2*. The error bars represent the SD of three replicates. The experiments were performed three times with similar results.

doi:10.1371/journal.pgen.1005584.g005

above). Heat-induced aggregation of CS was inhibited by HSP90 (Fig 6F), consistent with the results of previous study [37]. IBR5 showed a weaker but more significant effect than HSP90 on the inhibition of CS aggregation. When IBR5 was incubated with CS at 43°C, the aggregation of CS was partially suppressed in a dose-dependent manner (Fig 6E). This result indicates that IBR5 protects proteins against aggregation *in vitro*.

Genetic and physical interactions between IBR5 and SNC1

The TIR domain of CHS3 shares amino acid similarity with TIR-NB-LRR R proteins SNC1 and RPP4 (S4 Fig). Gain-of-function mutants of *SNC1* (*snc1-1* and *bal/snc1-2*) activate the defense response in a temperature-dependent manner [6,38]. The loss of *BON1* function in *Arabidopsis* leads to temperature-sensitive growth and autoimmune phenotypes resulting from the activation of SNC1 [6]. Phenotype analyses showed that the *bon1-1 ibr5-3* (*bon1 ibr5*) and *bal ibr5-3* (*bal ibr5*) double mutants were slightly larger than the *bon1-1* and *bal* single mutants (Fig 7A and 7B). Moreover, the cell death in *bon1 ibr5* and *bal ibr5* was reduced (Fig 7C). Consistently,

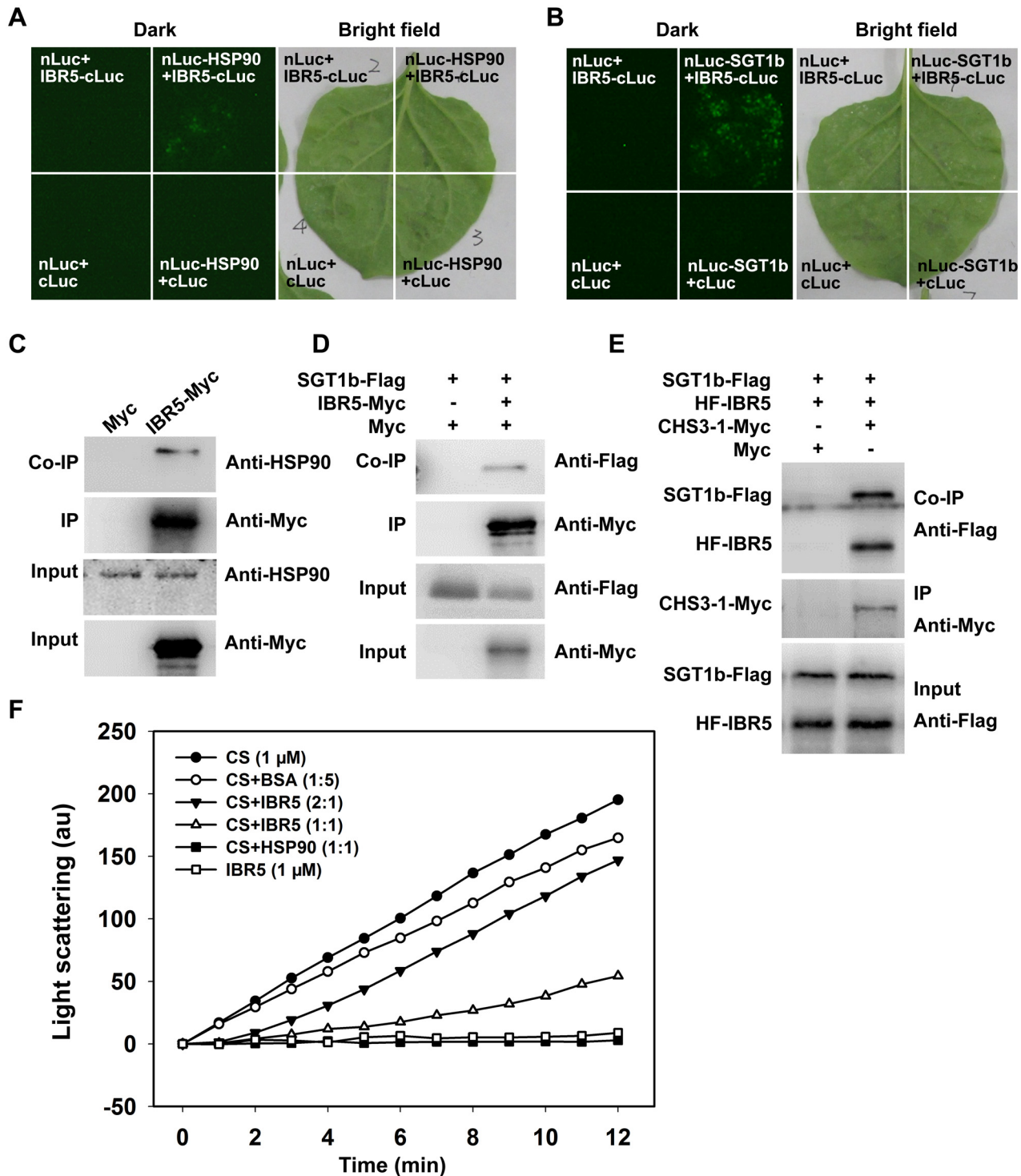


Fig 6. Interaction of IBR5 with HSP90 and SGT1b. (A) Interaction of IBR5 with HSP90 as revealed via firefly luciferase complementation imaging assay in *N. benthamiana* leaves. nLuc+cLuc-IBR5, HSP90-nLuc+cLuc, and nLuc+cLuc were used as negative controls. (B) Interaction of IBR5 with SGT1b as revealed by a firefly luciferase complementation imaging assay in *N. benthamiana* leaves. nLuc+cLuc-IBR5, SGT1b-nLuc+cLuc, and nLuc+cLuc were used as negative controls. (C) Co-immunoprecipitation of IBR5 and HSP90. Total protein was extracted from 2-week-old transgenic seedlings expressing *Super:IBR5-Myc* or *Super:Myc*. Anti-Myc antibody was used for immunoprecipitation, and the immunoprecipitated proteins were analyzed by immunoblotting using an anti-HSP90 antibody. (D) Co-immunoprecipitation of IBR5 and SGT1b. Total protein was extracted from transgenic plants expressing *Super:Myc/Super:SGT1b-Flag* or *Super:IBR5-Myc/Super:SGT1b-Flag*. An anti-Myc antibody was used for immunoprecipitation, and the immunoprecipitated proteins were analyzed by immunoblotting using an anti-Flag antibody. (E) Interaction of CHS3 with IBR5 and SGT1b in plant. Total proteins were extracted from *N.*

benthamiana leaves transfected with 35S:HF-IBR5, Super:SGT1b-Flag and Super:CHS3-1-Myc, and were immunoprecipitated with anti-Myc antibody. The proteins from crude lysates (Input) and the immunoprecipitated proteins were detected using an anti-Flag antibody. (F) IBR5 can stabilize CS under thermally denaturing conditions. Citrate synthase (1 μ M) was incubated alone or with 5 μ M BSA (1:5), 0.5 μ M IBR5 (2:1), 1 μ M IBR5 (1:1) or 1 μ M HSP90 (1:1) at 43°C. The kinetics was determined by light scattering using a fluorescence spectrophotometer.

doi:10.1371/journal.pgen.1005584.g006

the expression of *PR1* and *PR2* genes in *bon1 ibr5* and *bal ibr5* was also lower than that in the *bon1-1* and *bal/snc1-2* mutants (Fig 7D). We also examined the basal defense response of *bon1 ibr5* and *bal ibr5* to *P.s.t.* DC3000. The pathogen resistance of *bon1-1* and *bal/snc1-2* mutants to *P.s.t.* DC3000 was slightly suppressed in the *ibr5-3* mutant (Fig 7E and 7F). These genetic data suggest that IBR5 is partially implicated in the SNC1-mediated defense response.

To further dissect the function of IBR5 on SNC1, we examined the expression of *SNC1* in the *ibr5-3* mutant. As shown in Fig 4E, the *SNC1* transcript levels in the *ibr5-3* mutant were much lower than those in Col, indicating that *SNC1* expression is positively regulated by IBR5. We next explored whether IBR5 physically interacts with SNC1. A yeast two-hybrid assay showed that IBR5 interacted with the TIR domain of SNC1 (Fig 8A). The interaction of IBR5 and full-length SNC1-1 (the mutated form of SNC1 containing the same mutation as the *snc1-1* mutant) was confirmed by a co-IP assay in *N. benthamiana* leaves (Fig 8B). Moreover, the protein level of SNC1-1-Myc increased when co-expressed with HF-IBR5 in *Arabidopsis* protoplasts (Fig 8C). Taken together, these data suggest that IBR5 might also promote SNC1 protein accumulation.

Our previous studies showed that the mutations in R protein CHS2/RPP4 or R-like protein CHS1 induce plant sensitivity and activate defense responses under chilling stress [7,8]. To investigate whether *ibr5* also suppresses the chilling sensitivity of *chs1-2* and *chs2-1/rpp4-1d*, we generated *chs1-2 ibr5-3* (*chs1 ibr5*) and *chs2-1 ibr5-4* (*chs2 ibr5*) double mutants. In terms of morphology and cell death, *chs1 ibr5* and *chs2 ibr5* mutants showed *chs1-2* and *chs2-1* single mutant phenotypes under chilling stress (S5A and S5B Fig). However, *PR1* expression in *chs1 ibr5* was partially suppressed, whereas the expression of this protein in *chs2 ibr5* was not obviously affected. A yeast two-hybrid assay showed that IBR5 did not interact with RPP4 (Fig 8A). We also examined the pathogen resistance of *ibr5* mutants to RPP4-specific *Hyaloperonospora arabidopsidis* (*H.a.*) *Emwa1*. As controls, Col was completely resistant to *H.a. Emwa1*, whereas *rpp4-r26*, which contains a mutation in *RPP4* resulting in the introduction of a stop codon in front of the LRR domain [32], was susceptible to *H.a. Emwa1* (S6 Fig). The *ibr5-3* and *ibr5-7* mutants showed complete resistance to *H.a. Emwa1* (S6 Fig), suggesting that IBR5 might not be involved in RPP4-mediated oomycete resistance.

IBR5 is involved in RPM1- and RPS4-mediated disease resistance

To examine whether basal defense was affected in the *ibr5* single mutant, we infected wild-type Col and *ibr5* mutants with virulent *P.s.t.* DC3000. The bacterial growth in *ibr5-3* and *ibr5-7* was comparable to that in wild-type plants, whereas as the control, *pad4-1*, supported 100 times more bacterial growth than the wild-type plants (Fig 9A), suggesting that IBR5 does not play an important role in basal defense.

As the role of CHS3 is compromised in the *ibr5* mutant, we further investigated whether IBR5 is required for other R-gene-mediated disease resistance. The *ibr5* mutants were inoculated with *P.s.t.* DC3000 carrying either *avrRpm1*, *avrRps4*, or *avrRpt2*. The *ibr5* mutants showed enhanced susceptibility to *P.s.t.* DC3000 (*avrRpm1*) and *P.s.t.* DC3000 (*avrRps4*) (Fig 9B and 9C). In contrast, no remarkable difference in the growth of *P.s.t.* DC3000 (*avrRpt2*) was detected between the *ibr5* mutants and wild-type Col (Fig 8D). As a control, *pad4-1* showed enhanced disease susceptibility to all three avirulent bacterial strains (Fig 9B, 9C and 9D). These results suggest that IBR5 might also contribute to disease resistance mediated by RPM1 and RPS4.

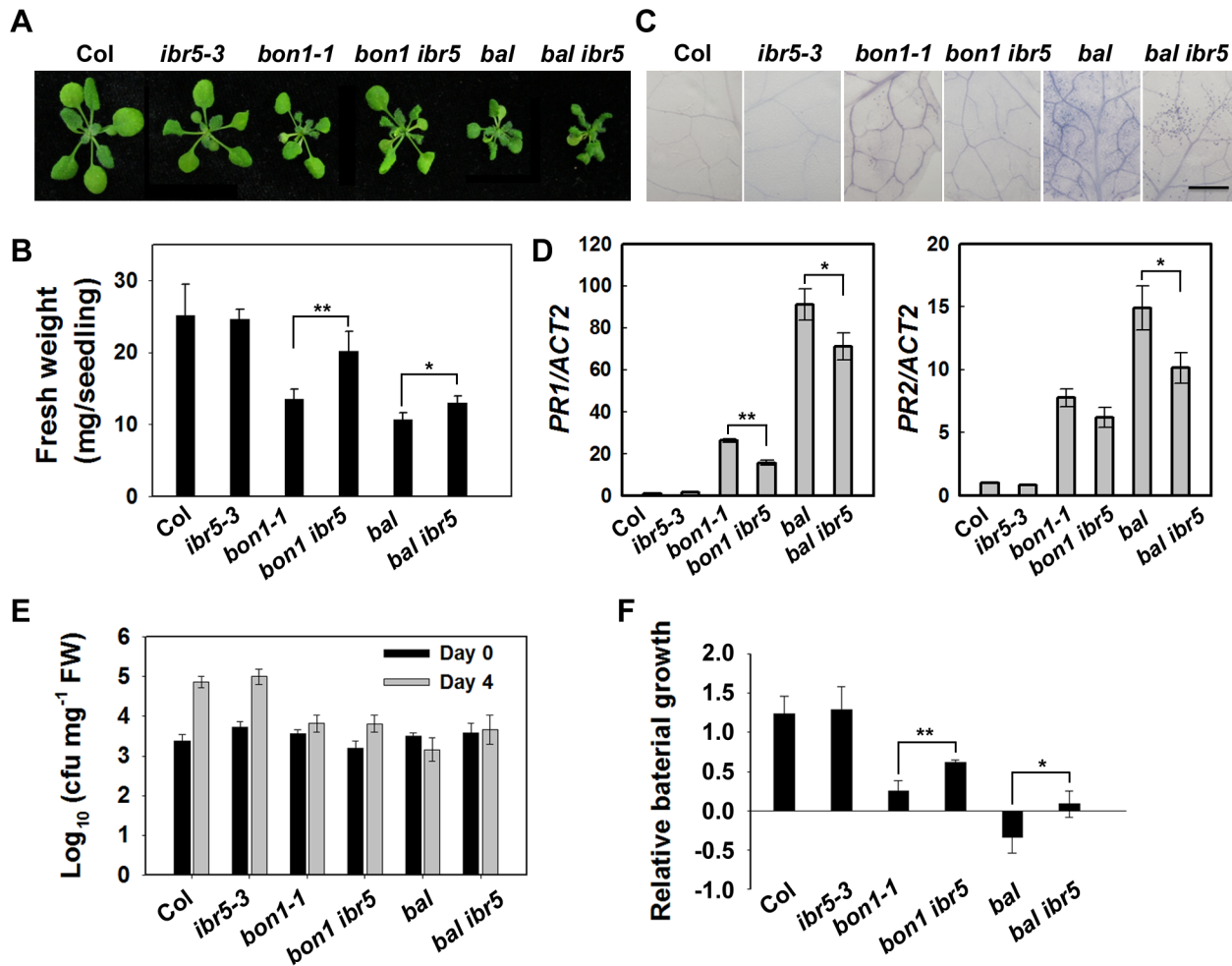


Fig 7. The defense phenotypes of *bon1-1 ibr5-3* and *bal ibr5-3*. Morphology of 3-week-old Col, *ibr5-3*, *bon1-1*, *bon1 ibr5-3*, *bal*, *bal ibr5-3* grown at 22°C. (B) Fresh weight of plants in (A). The error bars represent the SD of three replicates, and the asterisks indicate significant differences (***P* < 0.01, **P* < 0.05, *t*-test). (C) Trypan blue staining of leaves from the plants described in (A). Bar: 0.5 mm. The expression of *PR* genes in plants in (A). The error bars represent the SD of three replicates, and the asterisks indicate significant differences (***P* < 0.01, **P* < 0.05, *t*-test). (E) The effect of IBR5 on pathogen resistance of *bon1-1* and *bal* to *P.s.t.* DC3000. Three-week-old seedlings were dipped with *P.s.t.* DC3000 (OD₆₀₀ = 0.05), and leaves were taken immediately (day 0) and at day 4 after infection. The log-transformed values presented are the mean values of three replicates ± SD. The experiments were performed three times with similar results. (F) Relative bacterial growth of plants in (E) after infection with *P.s.t.* DC3000. The values are the ratios of bacteria number at day 4 to day 0. The error bars represent the SD of three replicates, and the asterisks indicate significant differences (***P* < 0.01, **P* < 0.05, *t*-test).

doi:10.1371/journal.pgen.1005584.g007

We next examined the expression of *RPM1* and *RPS4* in the *ibr5-3* mutant. The transcription levels of *RPM1* and *RPS4* were slightly down-regulated in the *ibr5-3* mutant compared with wild type plants (Fig 4F). Furthermore, we examined whether IBR5 interacts with TIR-NB-LRR protein *RPS4* or CC-NB-LRR protein *RPM1*. The results of a yeast two-hybrid assay showed that neither wild-type IBR5 nor mutated IBR5^{C129S} interacted with the TIR domain of *RPS4* or CC domain of *RPM1* (S7A Fig). However, interestingly, we observed the direct interaction of IBR5 and IBR5^{C129S} with *RPS4*-interacting protein *RRS1* [39] in yeast (S7B Fig). The results of additional co-IP assays showed that IBR5 could pull down *RPS4* (S7C Fig), suggesting that IBR5 might form a complex with *RPS4* and *RRS1*. In contrast, no interaction between IBR5 and *RPM1* was observed in plants (S7D Fig). Furthermore, no obvious change in the *RPM1* protein level was detected when IBR5 and *RPM1* were co-expressed (S7E Fig).

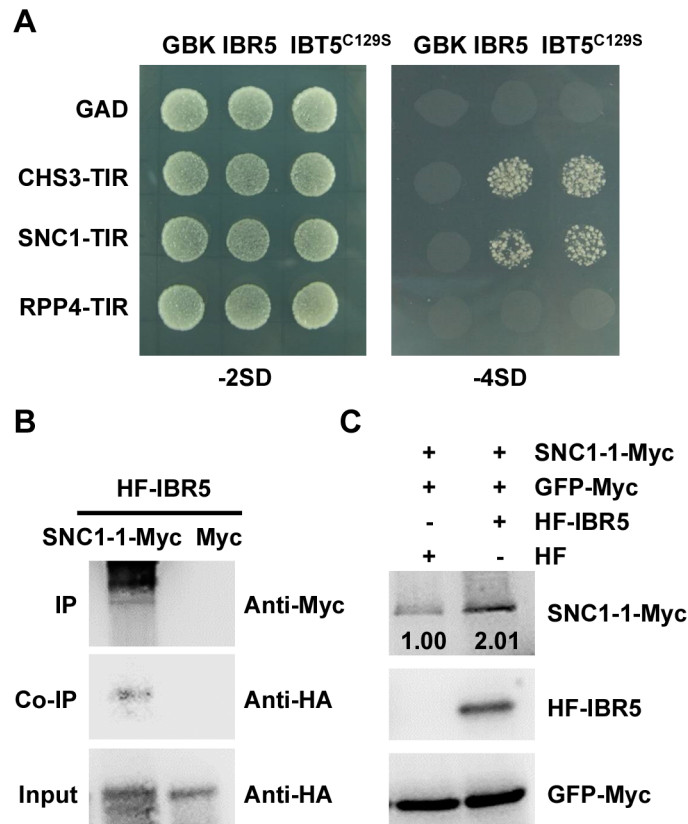


Fig 8. Interaction of IBR5 with SNC1 and RPP4. (A) Interaction of IBR5 with TIR domains of CHS3, SNC1 and RPP4 in yeast. The experiments were performed three times with similar results. (B) Interaction of IBR5 and full-length SNC1 *in vivo*. Total proteins were extracted from *N. benthamiana* leaves transfected with 35S:HF-IBR5 and Super:SNC1-1-Myc and were immunoprecipitated with an anti-Myc antibody. The proteins from crude lysates (Input) and the immunoprecipitated proteins were detected using an anti-HA antibody. (C) The effect of IBR5 on SNC1 protein level in *Arabidopsis* protoplasts. Super:SNC1-1-Myc and 35S:HF-IBR5 or 35S:HF constructs were co-expressed in *Arabidopsis* protoplasts. IBR5 was detected with anti-HA antibody and SNC1-1 was detected using an anti-Myc antibody. GFP-Myc construct was used as a control for transformation efficiency.

doi:10.1371/journal.pgen.1005584.g008

Discussion

CHS3 is involved in temperature-dependent defense responses [23]. In the present study, we identified *ibr5-7* as a suppressor of *chs3-1*. IBR5 interacts with CHS3 and HSP90/SGT1b chaperones to stabilize the CHS3 protein, thereby modulating temperature-dependent defense responses. In addition, IBR5 is involved in defense responses mediated by several other *R* genes, including *SNC1*, *RPS4* and *RPM1*.

IBR5 is a MAP kinase phosphatase (MKP) that dephosphorylates activated MAPKs [40,41]. Emerging evidence has shown that MKPs play important roles in modulating plant defense responses [41]. For example, the *mkp1* null mutation in the Col accession exhibits constitutive stress response phenotypes, causing a dwarf stature dependent on SNC1 [42]. However, it remains unclear whether the substrates of MKP1, MPK3 and MPK6 [42,43] are involved in the regulation of SNC1. Additional studies have revealed that MKP1 functions as a negative regulator of MPK6-mediated pathogen-associated molecular pattern (PAMP) responses and disease resistance [44]. The *mkp2* null mutant displays delayed symptoms of disease induced by *Ralstonia solanacearum*, and shows increased susceptibility to *Botrytis cinerea* [45]. MKP2 might

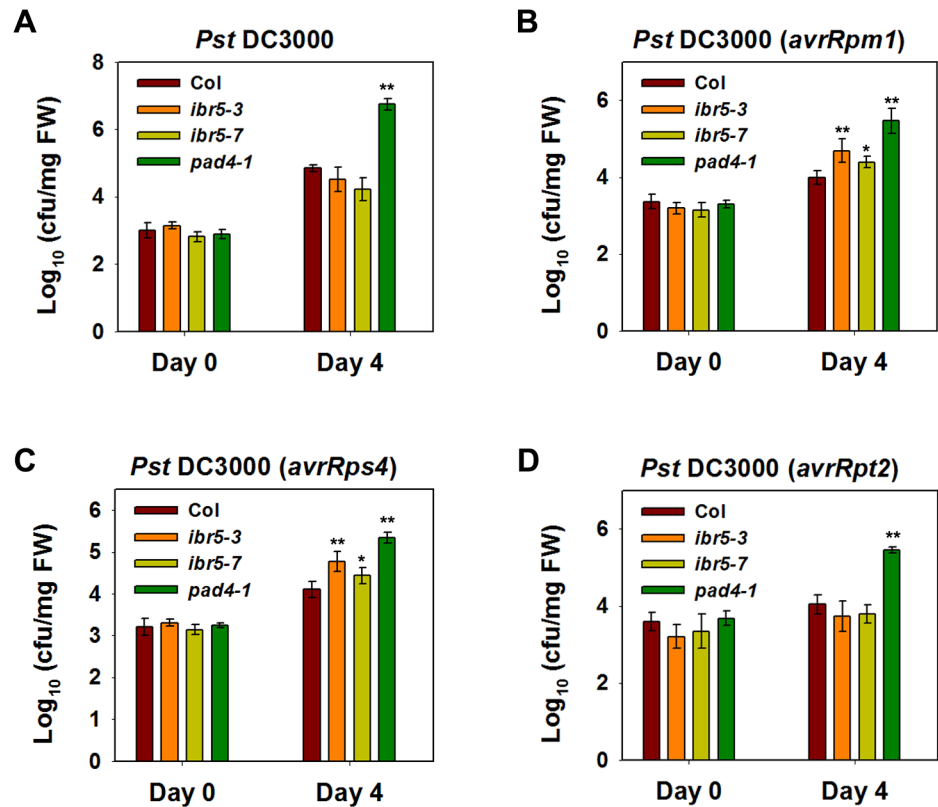


Fig 9. Pathogen resistance analysis of *ibr5* mutants. (A) Response of *ibr5* to *P.s.t.* DC3000. Three-week-old plants were dipped with *P.s.t.* DC 3000 ($OD_{600} = 0.05$), and leaves were taken immediately (day 0) and at day 4 after infection. The log-transformed values presented are the mean values of three replicates \pm SD. (B-D) Responses of *ibr5* to avirulent bacteria. Three-week-old plants were dipped with *P.s.t.* DC3000 (*avrRpt2*) (B), *P.s.t.* DC3000 (*avrRpm1*) (C) and *P.s.t.* DC3000 (*avrRps4*) (D) ($OD_{600} = 0.2$). In (A-D), the log-transformed values presented are the mean values of three replicates \pm SD, and the asterisks indicate significant differences compared with wild-type Col (** $P < 0.01$, * $P < 0.05$, *t*-test). All experiments were repeated at least three times with similar results.

doi:10.1371/journal.pgen.1005584.g009

regulate MPK3/MPK6 activity during different pathogen defense responses. Moreover, MKP2 reverses hypersensitive-like responses triggered by MPK6 upon plant treatment with fungal elicitors [45,46]. It is likely that these MKPs have negative functions in defense signaling pathways through their MPK substrates. The data obtained in the present study showed that the loss of *IBR5* function suppresses *chs3*-conferred, temperature-dependent defense responses and slightly weakens the autoimmunity of *bal/snc1-2*, a gain-of-function mutant of a TIR-NB-LRR protein *SNC1*. Moreover, resistance mediated by R proteins, such as *RPS4* and *RPM1*, is compromised in the *ibr5* mutants. These results suggest that *IBR5* plays a positive role in the ETI pathway mediated by multiple R proteins. Therefore, different MKPs play either positive or negative roles in plant immunity. As *IBR5* is a MAP kinase phosphatase, we also examined whether the dephosphorylation activity of *IBR5* is required for the regulation of *CHS3*. The inactive form of *IBR5* (*IBR5*^{C129S}) partially rescues the phenotype of *chs3 ibr5*, suggesting that the dephosphorylation activity of *IBR5* is necessary for the complete function of this protein in the *CHS3*-mediated defense response.

MPK12 is a substrate of *IBR5* [29], and the reduced expression of *MPK12* partially complements auxin, but not ABA insensitivity, in the *ibr5* mutant, suggesting that there might be other substrate(s) of *IBR5* involved in *IBR5*-mediated ABA responses [29]. In the present

study, the loss-of-function mutant *mpk12-3* displayed an auxin-sensitive phenotype (S8A, S8B and S8C Fig), similar to that of *mpk12 RNAi* lines [29]. However, *mpk12-3* cannot rescue the phenotype of *chs3 ibr5* (S8D Fig), indicating that the CHS3-mediated defense response does not require MPK12. Moreover, the mutant of auxin receptor *tir1* enhances the auxin insensitive phenotype of *ibr5*, implying that IBR5 is involved in the auxin response independently of the TIR1-mediated auxin signaling pathway [30]. Therefore, the role of IBR5 in R-mediated resistance might not occur through the function of IBR5 in the auxin response. *ibr5* mutant is shown to be insensitive to ABA, but the underlying mechanism is completely unknown [28]. ABA signaling plays a role in defense responses in a complicated manner. Recent studies have reported that the overexpression of ABA receptors maintains stomatal closure during *P.s.t.* DC3000 infections, leading to enhanced resistance after dipping, but enhanced susceptibility to the pathogen after infiltration [47]. In contrast, several ABA signaling mutants, such as *abi1* and *abi4*, do not exhibit prominent phenotypes under the *snc1-1* background or during pathogen infection [48]. The ABA-insensitive mutant *cpr22*, containing a deletion on two cyclic nucleotide-gated ion channel genes, shows constitutive *PR* gene expression, enhanced pathogen resistance and SA accumulation [49]. WRKY40, WRKY18, and WRKY60 play negative roles in ABA signaling [50]. The single and triple mutants show diverse phenotypes to different pathogens, as these mutants are more resistant to *P. syringae* but more susceptible to *B. cinerea* compared with the wild type [50]. Whether the role of IBR5 in the ABA response is involved in CHS3-mediated defense pathway remains unknown.

In plants, the TIR domain is indispensable for defense signal transduction [51]. For example, the transient expression of the TIR domain of RPS4 in *N. benthamiana* leaves triggers cell death in a manner dependent on both SGT1 and HSP90 [13,51]. The TIR domain of L6, a TIR-NB-LRR R protein in flax, forms a homodimer required for immune signaling [52]. A recent study showed that TIR domain heterodimerization is necessary to form a functional RRS1/RPS4 effector recognition complex [9], indicating the importance of the TIR domain of R proteins in signal recognition and transduction. Moreover, the TIR domain of R proteins interacts with other proteins [39,53–56]. In the present study, we observed that the TIR domain of CHS3 interacts with IBR5 *in vitro* and *in vivo*. The mutation of IBR5^{C129S} does not affect this interaction, suggesting that the dephosphatase activity of IBR5 is not a prerequisite for the interaction between IBR5 and CHS3. We also examined the interaction between IBR5 and four other TIR-NB-LRR R proteins: SNC1, RPP4, RPS4 and its interacting R protein RRS1 [39], and CC-NB-LRR, RPM1. Under these conditions, IBR5 interacts with SNC1 and RRS1/RPS4 in plant, but not with RPP4 and RPM1. Consistently, *ibr5* partially suppresses the cell death and *PR* gene expression in *bal/snc1-2* but does not suppress the expression of these proteins in *chs2/rpp4-1d*. These data suggest that IBR5 might specifically interact with certain TIR-NB-LRR proteins to regulate defense signaling. However, the mechanism underlying the involvement of IBR5 in defense responses mediated by the CC-type R protein remain unclear.

Increasing evidence has shown that HSP90, SGT1 and RAR1 form a protein complex with chaperone activity required for the proper folding and stabilization of R proteins [11,23,33,34,57–60]. In this complex, HSP90 and RAR1 increase R protein levels [57]. The phosphatase PP5 interacts with HSP90 and the tomato R protein I-2, and together with HSP90, PP5 acts as a co-chaperone [61]. In the present study, we found an interaction between the phosphatase IBR5 and the HSP90/SGT1B/RAR1 complex *in vivo*, suggesting that IBR5 complexes with these chaperone proteins and stabilizes CHS3. Increasing evidence further supports the notion: (1) The *in vitro* holdase activity of IBR5 indicates that this enzyme markedly inhibits temperature-dependent CS degradation. (2) The F1 progeny of *chs3 ibr5* and *chs3 hsp90* partially inhibits the *chs3* phenotype. Moreover, the *chs3 ibr5 hsp90* triple mutant is larger than both *chs3 hsp90* and *chs3 ibr5* and is reminiscent of the wild type. We speculate that

different complexes comprising IBR5 and HSP90 might play roles in CHS3-mediated signaling. This involvement might reflect the dosage effect of *IBR5* and *HSP90*. A similar mechanism was observed for the COI1 (CORONATINE INSENSITIVE 1) and HSP90 proteins in regulating RPM1-mediated disease resistance [62]. (3) *chs3*-dependent phenotypes are suppressed by *sgt1b*, *rar1* [23] and *hsp90.3-1*, indicating that HSP90, RAR1 and SGT1b are required for *CHS3* activation. (4) IBR5 interacts with the HSP90, SGT1b and CHS3 proteins *in vivo*. Collectively, these data show that IBR5 associates with HSP90/RAR1/SGT1b to stabilize the CHS3 protein. Because SGT1b interacts with a core component of the SKP1-CULLIN1-F-box (SCF) E3 ligase complex, S-phase kinase-associated protein 1 (SKP1), SGT1b has been considered as a subunit of the SCF complex [63,64]. Recent studies have shown that SNC1 is degraded by the SCF^{CPR1} complex [65,66]. In a protein-protein interactome study, IBR5 was also shown to interact with SKP1 [67]. These results suggest that IBR5, in concert with HSP90/SGT1B proteins, might affect the function of SCF ubiquitin ligase complexes, thereby regulating the ubiquitination and degradation of some R proteins. Further studies will elucidate the molecular mechanisms underlying the roles of IBR5 in R-mediated defense responses.

Materials and Methods

Plant materials and growth conditions

Arabidopsis thaliana Col-0, *chs3-1* [23], *ibr5-3* [29], *pad4-1* [68], *hsp90.3-1*, *rpp4-r26* [32], and *mpk12-3* (SAIL_543_F07) were used in this study. Plants were grown in soil or on Murashige and Skoog (MS) medium containing 2% (w/v) Suc and 0.8% (w/v) agar at 16°C or 22°C with a 16-h light/8-h dark cycle under white light. Salicylic acid measurement and were described previously [23].

Suppressor screening and map-based cloning of *SUC5*

The suppressors of *chs3-1* were screened and mapped as described previously [23]. Approximately 200 plants with *chs3-1* background with wild-type morphology at 16°C were used for mapping to a 500-kb region between markers F3C11 and F5G3. Full length genomic DNA of candidate genes was amplified by PCR and sequenced to find the mutant site. To confirm the mutated gene, genomic complementation and T-DNA insertion mutant were used.

Trypan blue staining and DAB staining

Trypan blue and DAB staining was performed as previously described [69,70].

Pathogen resistance assay

The pathogen resistance assay on *Pseudomonas syringae* pv *tomato* (*P.s.t.*) strain DC3000 was performed as described previously [32]. Briefly, 3-week-old plants were dipped by the bacterial suspension containing 10 mM MgCl₂ and 0.025% Silwet L-77. The concentrations of pathogen for virulent strain (*P.s.t.* DC3000) and avirulent strains (*P.s.t.* DC3000 with *avrRmp1*, *avrRpt2* and *avrRps4*) are OD₆₀₀ of 0.05 and 0.2, respectively. The dipped leaves were collected at 2 hour and 4 day post-inoculation. Three replicate samples were collected to measure the resistance to pathogen.

qRT-PCR analysis

Total RNA isolated from 2-week-old plants grown at 22°C or 3-week-old plants grown at 16°C using TRIzol reagent (Invitrogen). The quantitative real-time PCR was performed using a

SYBR Green PCR Master Mix kit (Takara). The relative expression levels were calculated as described (Huang et al., 2010). Gene-specific primers were listed in [S1 Table](#).

Plasmid construction and plant transformation

To obtain the *IBR5::IBR5* construct, the genome fragment of *IBR5* (from ~2kb upstream of ATG to stop codon) was amplified and cloned into pCAMBIA1300 vector. To generate *Super:IBR5* and *Super:SGT1b* constructs, cDNAs of *IBR5* and *SGT1b* were amplified and cloned into the pSuper1300-Myc/GFP/Flag vectors containing a Super promoter.

To generate *Super:CHS3-1-Myc*, *Super:SNC1-1-Myc*, *Super:RPM1-Myc* and *Super:RPS4-Myc*, genomic DNA of *chs3-1*, *snc1-1*, *RPM1* and *RPS4* were amplified and cloned into the pSuper1300-Myc vectors containing a Super promoter. The primers were listed in [S1 Table](#).

Agrobacterium tumefaciens strain of GV3101 carrying different constructs was transformed into wild-type or mutant plants via standard floral dipping method [71].

Yeast two-hybrid assay

To create bait and prey plasmids, fragments were amplified by different primers and cloned into pGBKT7 and pGADT7. All primer sequences are listed in [S1 Table](#). Bait and prey plasmids were co-transformed into yeast strain AH109. Yeast strains containing the bait and prey plasmids were cultured in SD-Trp-Leu liquid medium to $OD_{600} = 0.4-0.6$. Interaction was tested on SD-Trp-Leu-His-Ade medium.

LCI assay

cDNAs of *HSP90* and *SGT1b* were amplified and cloned into nLuc vector. *IBR5* cDNA was amplified and cloned into cLuc vector. *A. tumefaciens* strain GV3101 containing different constructs was infiltrated into *N. benthamiana* leaves according to the protocol described previously [72]. Firefly Luciferase Complementation Imaging (LCI) assay was performed as described [73].

Thermal aggregation assay

To clone the *IBR5-His* construct, *IBR5* cDNA was amplified and cloned into pQE80L vector. *HSP90* fragment was amplified and cloned into pMalC2 vector. The thermal aggregation assay was performed as described [74] with some modifications. Citrate synthase from porcine heart (Sigma-Aldrich) was used as substrate. Light scattering was measured by a thermostatically controlled fluorescence spectrophotometer (F-7000). Proteins were diluted by 40 mM HEPES/KOH (pH 7.5) and the reaction temperature was kept at 43°C.

Coimmunoprecipitation

The plasmids were purified and transformed into *Arabidopsis* mesophyll protoplasts [75] or *N. benthamiana* leaves [72]. Proteins were extracted with extracting buffer containing 150 mM NaCl, 10 mM Tris-HCl pH 7.6, 2 mM EDTA, 0.5% NP-40 and 1 x protease inhibitor cocktail (Roche). The protein extracts were then incubated with anti-Myc beads (Sigma-Aldrich) at 4°C for 2 hour. After washing five times with extraction buffer, the samples were used for immunoblotting with anti-HA (Sigma-Aldrich) or anti-Flag (Sigma-Aldrich) antibodies.

Supporting Information

S1 Fig. The responses of *ibr5* mutants to auxin. Auxin responses of wild type Col, *chs3-1*, *ibr5-3*, *ibr5-7*, and *chs3-1 ibr5-7*. Four-day-old seedlings grown on MS medium with 10 μ M

IBA, 10 nM IAA, or 50 nM 2,4-D. The relative root length was calculated as root length of seedling grown with hormones versus control (without hormones).

(TIF)

S2 Fig. Subcellular localization of IBR5 and CHS3 proteins. (A) Subcellular localization of IBR5 in *Arabidopsis* protoplasts. The *Super:IBR5-GFP* and *Super:GFP* plasmids were transformed into *Arabidopsis* protoplasts, and the signals were detected using a confocal laser-scanning microscope. The green fluorescence signals, chlorophyll red autofluorescence, an overlay of the green and red signals, and bright-field images are shown. Bars: 20 μ m. (B) The subcellular localization of IBR5 and CHS3 proteins in the roots of *Super:IBR5-GFP* and *CHS3:chs3-2D-GFP* transgenic plants. Bar: 100 μ m.

(TIF)

S3 Fig. Inteaction of SGT1b and CHS3 in plant. (A) Inteaction of SGT1b and TIR domain of CHS3 *in vivo*. *Super:CHS3-TIR-Myc* or *Super:Myc* was co-expressed with *Super:SGT1b-Flag* in *Arabidopsis* protoplasts. An anti-Myc antibody was used for immunoprecipitation and the immunoprecipitated proteins were analyzed by immunoblotting using an anti-FLAG antibody. (B) Interaction of SGT1b and full-length CHS3 *in vivo*. *Super:SGT1b-Flag* and *Super:CHS3-1-Myc* or *Super:Myc* was co-expressed with *Super:SGT1b-Flag* in *N. benthamiana* leaves. An anti-Myc antibody was used for immunoprecipitation and the immunoprecipitated proteins were analyzed by immunoblotting using an anti-FLAG antibody.

(TIF)

S4 Fig. Alignment of TIR domains of CHS3, RPP4 and SNC1 proteins.

(TIF)

S5 Fig. Phenotypes of *chs1 ibr5* and *chs2 ibr5* mutants. (A) Morphology (top panel) and trypan blue (bottom panel) staining of 4-week-old Col, *ibr5-3*, *chs1-2*, and *chs1 ibr5*. Ten-day-old seedlings grown at 22°C were transferred to 16°C for additional 3 weeks. Bar: 200 μ m. (B) The expression of *PR* genes in plants in (A). The error bars represent the SD of three replicates. (C) Morphology (top panel) and trypan blue (bottom panel) staining of Col, *ibr5-7*, *chs2-1* and *chs2 ibr5*. Two-week-old seedlings grown at 22°C were transferred to 4°C for an additional week. Bar: 200 μ m. (D) Expression of *PR* genes in plants in (C). The error bars represent the SD of three replicates.

(TIF)

S6 Fig. Quantification of *Hyaloperonospora arabidopsidis* (*H.a.*) Emwa1 sporulation on wild type, *ibr5-3*, *ibr5-7* and *rpp4-r26* plants. 2-week-old seedlings were sprayed with *H.a.* Emwa1 at a concentration of 200,000 spores per 1 mL of water. The spores were quantified 7 day after inoculation. The data are mean values of five replicates \pm SD. The experiment was repeated three times with similar results.

(TIF)

S7 Fig. Interaction of IBR5 with RPS1 and RPM1. (A, B) Interaction of IBR5 and RPS4, RPM1 (A) and RRS1 (B) in yeast. TIR domains of RPS4, RPM1 (A), CHS3 and RRS1 (B) were fused with the pGADT7 vector. IBR5 and mutated IBR5^{C129S} were fused with the pGBKT7 vector. The constructs were transformed into AH109 yeast cells and spotted onto SD media lacking Trp and Leu (-2SD) or lacking Trp, Leu, His and Ade (-4SD). The experiments were performed three times with similar results. (A, B) Interaction of IBR5 with TIR domains of RPS4, RPM1 (A), CHS3 and RRS1 (B) in yeast. The experiments were performed three times with similar results. (C) Interaction of IBR5 and full-length RPS4 *in vivo*. Total proteins were extracted from *N. benthamiana* leaves transfected with 35S: *HF-IBR5* and *Super:RPS4-Myc* or

Super:Myc, and were immunoprecipitated with anti-Myc antibody. The proteins from crude lysates (Input) and the immunoprecipitated proteins were detected using an anti-HA antibody. (D) Interaction of IBR5 and full-length RPM1 *in vivo*. Total proteins were extracted from *N. benthamiana* leaves transfected with 35S:HF-IBR5 and *Super:RPM1-Myc* or *Super:Myc*, and were immunoprecipitated with anti-Myc antibody. The proteins from crude lysates (Input) and the immunoprecipitated proteins were detected using an anti-HA antibody. (E) The effect of IBR5 on RPM1 protein level in *Arabidopsis* protoplasts. *Super:RPM1-Myc* and 35S:HF-IBR5 or 35S:HF constructs were co-expressed in *Arabidopsis* protoplasts. IBR5 was detected with anti-HA antibody and RPM1 was detected using an anti-Myc antibody. The *GFP-Myc* construct was used as a control for transformation efficiency. (TIF)

S8 Fig. *chs3 ibr5* phenotype is not rescued by *mpk12* mutant. (A) Diagram of genomic fragment of the *MPK12* gene. The exons are presented as dark blue boxes, UTR regions are presented as light blue boxes, and intron regions are presented as lines. The position of *mpk12-3* (SAIL_543_F07) is shown. (B) RT-PCR analysis of *MPK12* in Col and *mpk12*. The *EF1 α* was used as a control. (C) Responses of *MPK12-RNAi* and *mpk12-3* mutants to auxin. (D) Phenotypes of Col, *chs3-1*, *ibr5-7*, *chs3 ibr5*, *mpk12*, *chs3 mpk12* and *chs3 ibr5 mpk12* grown in soil at 16°C for 3 weeks. (TIF)

S1 Table. Gene-specific primers used in this study. (DOC)

Acknowledgments

We thank Jianmin Zhou (Institute of Genetics and Developmental Biology, Chinese Academy of Sciences) for kindly providing plasmids for LCI.

Author Contributions

Conceived and designed the experiments: SY JL HY. Performed the experiments: JL HY FB XZ KA. Analyzed the data: JL HY YZ. Wrote the paper: SY JL.

References

1. Hua J (2013) Modulation of plant immunity by light, circadian rhythm, and temperature. *Curr Opin Plant Biol* 16: 406–413. doi: [10.1016/j.pbi.2013.06.017](https://doi.org/10.1016/j.pbi.2013.06.017) PMID: [23856082](https://pubmed.ncbi.nlm.nih.gov/23856082/)
2. Alcazar R, Garcia AV, Parker JE, Reymond M (2009) Incremental steps toward incompatibility revealed by *Arabidopsis* epistatic interactions modulating salicylic acid pathway activation. *Proc Natl Acad Sci U S A* 106: 334–339. doi: [10.1073/pnas.0811734106](https://doi.org/10.1073/pnas.0811734106) PMID: [19106299](https://pubmed.ncbi.nlm.nih.gov/19106299/)
3. de Jong CF, Takken FL, Cai X, de Wit PJ, Joosten MH (2002) Attenuation of Cf-mediated defense responses at elevated temperatures correlates with a decrease in elicitor-binding sites. *Mol Plant Microbe Interact* 15: 1040–1049. PMID: [12437302](https://pubmed.ncbi.nlm.nih.gov/12437302/)
4. Li Y, Pennington BO, Hua J (2009) Multiple R-like genes are negatively regulated by BON1 and BON3 in *Arabidopsis*. *Mol Plant Microbe Interact* 22: 840–848. doi: [10.1094/MPMI-22-7-0840](https://doi.org/10.1094/MPMI-22-7-0840) PMID: [19522566](https://pubmed.ncbi.nlm.nih.gov/19522566/)
5. Xiao S, Charoenwattana P, Holcombe L, Turner JG (2003) The *Arabidopsis* genes *RPW8.1* and *RPW8.2* confer induced resistance to powdery mildew diseases in tobacco. *Mol Plant Microbe Interact* 16: 289–294. PMID: [12744457](https://pubmed.ncbi.nlm.nih.gov/12744457/)
6. Yang S, Hua J (2004) A haplotype-specific Resistance gene regulated by BONZAI1 mediates temperature-dependent growth control in *Arabidopsis*. *Plant Cell* 16: 1060–1071. PMID: [15031411](https://pubmed.ncbi.nlm.nih.gov/15031411/)
7. Huang X, Li J, Bao F, Zhang X, Yang S (2010) A gain-of-function mutation in the *Arabidopsis* disease resistance gene *RPP4* confers sensitivity to low temperature. *Plant Physiol* 154: 796–809. doi: [10.1104/pp.110.157610](https://doi.org/10.1104/pp.110.157610) PMID: [20699401](https://pubmed.ncbi.nlm.nih.gov/20699401/)

8. Wang Y, Zhang Y, Wang Z, Zhang X, Yang S (2013) A missense mutation in CHS1, a TIR-NB protein, induces chilling sensitivity in Arabidopsis. *Plant J* 75: 553–565. doi: [10.1111/tbj.12232](https://doi.org/10.1111/tbj.12232) PMID: [23651299](https://pubmed.ncbi.nlm.nih.gov/23651299/)
9. Cheng C, Gao X, Feng B, Sheen J, Shan L, et al. (2013) Plant immune response to pathogens differs with changing temperatures. *Nat Commun* 4: 2530. doi: [10.1038/ncomms3530](https://doi.org/10.1038/ncomms3530) PMID: [24067909](https://pubmed.ncbi.nlm.nih.gov/24067909/)
10. Kadota Y, Shirasu K (2012) The HSP90 complex of plants. *Biochim Biophys Acta* 1823: 689–697. doi: [10.1016/j.bbamcr.2011.09.016](https://doi.org/10.1016/j.bbamcr.2011.09.016) PMID: [22001401](https://pubmed.ncbi.nlm.nih.gov/22001401/)
11. Hubert DA, Tornero P, Belkhadir Y, Krishna P, Takahashi A, et al. (2003) Cytosolic HSP90 associates with and modulates the Arabidopsis RPM1 disease resistance protein. *EMBO J* 22: 5679–5689. PMID: [14592967](https://pubmed.ncbi.nlm.nih.gov/14592967/)
12. Liu Y, Burch-Smith T, Schiff M, Feng S, Dinesh-Kumar SP (2004) Molecular chaperone Hsp90 associates with resistance protein N and its signaling proteins SGT1 and Rar1 to modulate an innate immune response in plants. *J Biol Chem* 279: 2101–2108. PMID: [14583611](https://pubmed.ncbi.nlm.nih.gov/14583611/)
13. Zhang Y, Dorey S, Swiderski M, Jones JD (2004) Expression of *RPS4* in tobacco induces an AvrRps4-independent HR that requires EDS1, SGT1 and HSP90. *Plant J* 40: 213–224. PMID: [15447648](https://pubmed.ncbi.nlm.nih.gov/15447648/)
14. Holt BF 3rd, Belkhadir Y, Dangl JL (2005) Antagonistic control of disease resistance protein stability in the plant immune system. *Science* 309: 929–932. PMID: [15976272](https://pubmed.ncbi.nlm.nih.gov/15976272/)
15. Li Y, Li S, Bi D, Cheng YT, Li X, et al. (2010) SRFR1 negatively regulates plant NB-LRR resistance protein accumulation to prevent autoimmunity. *PLoS Pathog* 6: e1001111. doi: [10.1371/journal.ppat.1001111](https://doi.org/10.1371/journal.ppat.1001111) PMID: [20862316](https://pubmed.ncbi.nlm.nih.gov/20862316/)
16. Huang S, Monaghan J, Zhong X, Lin L, Sun T, et al. (2014) HSP90s are required for NLR immune receptor accumulation in Arabidopsis. *Plant J* 79: 427–439. doi: [10.1111/tbj.12573](https://doi.org/10.1111/tbj.12573) PMID: [24889324](https://pubmed.ncbi.nlm.nih.gov/24889324/)
17. Li Y, Tessaro MJ, Li X, Zhang Y (2010) Regulation of the expression of plant resistance gene SNC1 by a protein with a conserved BAT2 domain. *Plant Physiol* 153: 1425–1434. doi: [10.1104/pp.110.156240](https://doi.org/10.1104/pp.110.156240) PMID: [20439546](https://pubmed.ncbi.nlm.nih.gov/20439546/)
18. Zhang Y, Li X (2005) A putative nucleoporin 96 Is required for both basal defense and constitutive resistance responses mediated by suppressor of *npr1-1, constitutive 1*. *Plant Cell* 17: 1306–1316. PMID: [15772285](https://pubmed.ncbi.nlm.nih.gov/15772285/)
19. Cheng YT, Germain H, Wiermer M, Bi D, Xu F, et al. (2009) Nuclear pore complex component MOS7/Nup88 is required for innate immunity and nuclear accumulation of defense regulators in Arabidopsis. *Plant Cell* 21: 2503–2516. doi: [10.1105/tpc.108.064519](https://doi.org/10.1105/tpc.108.064519) PMID: [19700630](https://pubmed.ncbi.nlm.nih.gov/19700630/)
20. Zhu Z, Xu F, Zhang Y, Cheng YT, Wiermer M, et al. (2010) Arabidopsis resistance protein SNC1 activates immune responses through association with a transcriptional corepressor. *Proc Natl Acad Sci U S A* 107: 13960–13965. doi: [10.1073/pnas.1002828107](https://doi.org/10.1073/pnas.1002828107) PMID: [20647385](https://pubmed.ncbi.nlm.nih.gov/20647385/)
21. Huang Y, Minaker S, Roth C, Huang S, Hieter P, et al. (2014) An E4 ligase facilitates polyubiquitination of plant immune receptor resistance proteins in Arabidopsis. *Plant Cell* 26: 485–496. doi: [10.1105/tpc.113.119057](https://doi.org/10.1105/tpc.113.119057) PMID: [24449689](https://pubmed.ncbi.nlm.nih.gov/24449689/)
22. Cheng YT, Li Y, Huang S, Huang Y, Dong X, et al. (2011) Stability of plant immune-receptor resistance proteins is controlled by SKP1-CULLIN1-F-box (SCF)-mediated protein degradation. *Proc Natl Acad Sci U S A* 108: 14694–14699. doi: [10.1073/pnas.1105685108](https://doi.org/10.1073/pnas.1105685108) PMID: [21873230](https://pubmed.ncbi.nlm.nih.gov/21873230/)
23. Yang H, Shi Y, Liu J, Guo L, Zhang X, et al. (2010) A mutant CHS3 protein with TIR-NB-LRR-LIM domains modulates growth, cell death and freezing tolerance in a temperature-dependent manner in Arabidopsis. *Plant J* 63: 283–296. doi: [10.1111/j.1365-313X.2010.04241.x](https://doi.org/10.1111/j.1365-313X.2010.04241.x) PMID: [20444230](https://pubmed.ncbi.nlm.nih.gov/20444230/)
24. Bi D, Johnson K, Huang Y, Zhu Z, Li X, et al. (2011) Mutations in an atypical TIR-NB-LRR-LIM resistance protein confers autoimmunity. *Front Plant Sci* doi: [10.3389/fpls.2011.00071](https://doi.org/10.3389/fpls.2011.00071)
25. Austin MJ, Muskett P, Kahn K, Feys BJ, Jones JD, et al. (2002) Regulatory role of SGT1 in early R gene-mediated plant defenses. *Science* 295: 2077–2080. PMID: [11847308](https://pubmed.ncbi.nlm.nih.gov/11847308/)
26. Shirasu K, Lahaye T, Tan MW, Zhou F, Azevedo C, et al. (1999) A novel class of eukaryotic zinc-binding proteins is required for disease resistance signaling in barley and development in *C. elegans*. *Cell* 99: 355–366. PMID: [10571178](https://pubmed.ncbi.nlm.nih.gov/10571178/)
27. Tornero P, Merritt P, Sadanandom A, Shirasu K, Innes RW, et al. (2002) RAR1 and NDR1 contribute quantitatively to disease resistance in Arabidopsis, and their relative contributions are dependent on the R gene assayed. *Plant Cell* 14: 1005–1015. PMID: [12034893](https://pubmed.ncbi.nlm.nih.gov/12034893/)
28. Monroe-Augustus M, Zolman BK, Bartel B (2003) IBR5, a dual-specificity phosphatase-like protein modulating auxin and abscisic acid responsiveness in Arabidopsis. *Plant Cell* 15: 2979–2991. PMID: [14630970](https://pubmed.ncbi.nlm.nih.gov/14630970/)
29. Lee JS, Wang S, Sritubtim S, Chen JG, Ellis BE (2009) Arabidopsis mitogen-activated protein kinase MPK12 interacts with the MAPK phosphatase IBR5 and regulates auxin signaling. *Plant J* 57: 975–985. doi: [10.1111/j.1365-313X.2008.03741.x](https://doi.org/10.1111/j.1365-313X.2008.03741.x) PMID: [19000167](https://pubmed.ncbi.nlm.nih.gov/19000167/)

30. Strader LC, Monroe-Augustus M, Bartel B (2008) The IBR5 phosphatase promotes Arabidopsis auxin responses through a novel mechanism distinct from TIR1-mediated repressor degradation. *BMC Plant Biol* 8: 41. doi: [10.1186/1471-2229-8-41](https://doi.org/10.1186/1471-2229-8-41) PMID: [18423007](https://pubmed.ncbi.nlm.nih.gov/18423007/)
31. Pearl LH, Prodromou C (2006) Structure and mechanism of the Hsp90 molecular chaperone machinery. *Annu Rev Biochem* 75: 271–294. PMID: [16756493](https://pubmed.ncbi.nlm.nih.gov/16756493/)
32. Bao F, Huang X, Zhu C, Zhang X, Li X, et al. (2014) Arabidopsis HSP90 protein modulates RPP4-mediated temperature-dependent cell death and defense responses. *New Phytol* 202: 1320–1334. doi: [10.1111/nph.12760](https://doi.org/10.1111/nph.12760) PMID: [24611624](https://pubmed.ncbi.nlm.nih.gov/24611624/)
33. Liu Y, Burch-Smith T, Schiff M, Feng S, Dinesh-Kumar SP (2004) Molecular chaperone Hsp90 associates with resistance protein N and its signaling proteins SGT1 and Rar1 to modulate an innate immune response in plants. *J Biol Chem* 279: 2101–2108. PMID: [14583611](https://pubmed.ncbi.nlm.nih.gov/14583611/)
34. Takahashi A, Casais C, Ichimura K, Shirasu K (2003) HSP90 interacts with RAR1 and SGT1 and is essential for RPS2-mediated disease resistance in Arabidopsis. *Proc Natl Acad Sci U S A* 100: 11777–11782. PMID: [14504384](https://pubmed.ncbi.nlm.nih.gov/14504384/)
35. Kadota Y, Amigues B, Ducassou L, Madaoui H, Ochsenbein F, et al. (2008) Structural and functional analysis of SGT1-HSP90 core complex required for innate immunity in plants. *EMBO Rep* 9: 1209–1215. doi: [10.1038/embor.2008.185](https://doi.org/10.1038/embor.2008.185) PMID: [18833289](https://pubmed.ncbi.nlm.nih.gov/18833289/)
36. Schumacher RJ, Hansen WJ, Freeman BC, Alnemri E, Litwack G, et al. (1996) Cooperative action of Hsp70, Hsp90, and DnaJ proteins in protein renaturation. *Biochemistry* 35: 14889–14898. PMID: [8942653](https://pubmed.ncbi.nlm.nih.gov/8942653/)
37. Shaknovich R, Shue G, Kohtz DS (1992) Conformational activation of a basic helix-loop-helix protein (MyoD1) by the C-terminal region of murine HSP90 (HSP84). *Mol Cell Biol* 12: 5059–5068. PMID: [1406681](https://pubmed.ncbi.nlm.nih.gov/1406681/)
38. Zhang Y, Goritschnig S, Dong X, Li X (2003) A gain-of-function mutation in a plant disease resistance gene leads to constitutive activation of downstream signal transduction pathways in suppressor of *npr1-1*, *constitutive 1*. *Plant Cell* 15: 2636–2646. PMID: [14576290](https://pubmed.ncbi.nlm.nih.gov/14576290/)
39. Williams SJ, Sohn KH, Wan L, Bernoux M, Sarris PF, et al. (2014) Structural basis for assembly and function of a heterodimeric plant immune receptor. *Science* 344: 299–303. doi: [10.1126/science.1247357](https://doi.org/10.1126/science.1247357) PMID: [24744375](https://pubmed.ncbi.nlm.nih.gov/24744375/)
40. Dickinson RJ, Keyse SM (2006) Diverse physiological functions for dual-specificity MAP kinase phosphatases. *J Cell Sci* 119: 4607–4615. PMID: [17093265](https://pubmed.ncbi.nlm.nih.gov/17093265/)
41. Bartels S, Gonzalez Besteiro MA, Lang D, Ulm R (2010) Emerging functions for plant MAP kinase phosphatases. *Trends Plant Sci* 15: 322–329. doi: [10.1016/j.tplants.2010.04.003](https://doi.org/10.1016/j.tplants.2010.04.003) PMID: [20452268](https://pubmed.ncbi.nlm.nih.gov/20452268/)
42. Bartels S, Anderson JC, Gonzalez Besteiro MA, Carreri A, Hirt H, et al. (2009) MAP kinase phosphatase1 and protein tyrosine phosphatase1 are repressors of salicylic acid synthesis and SNC1-mediated responses in Arabidopsis. *Plant Cell* 21: 2884–2897. doi: [10.1105/tpc.109.067678](https://doi.org/10.1105/tpc.109.067678) PMID: [19789277](https://pubmed.ncbi.nlm.nih.gov/19789277/)
43. Ulm R, Ichimura K, Mizoguchi T, Peck SC, Zhu T, et al. (2002) Distinct regulation of salinity and genotoxic stress responses by Arabidopsis MAP kinase phosphatase 1. *EMBO J* 21: 6483–6493. PMID: [12456655](https://pubmed.ncbi.nlm.nih.gov/12456655/)
44. Anderson JC, Bartels S, Gonzalez Besteiro MA, Shahollari B, Ulm R, et al. (2011) Arabidopsis MAP Kinase Phosphatase 1 (AtMKP1) negatively regulates MPK6-mediated PAMP responses and resistance against bacteria. *Plant J* 67: 258–268. doi: [10.1111/j.1365-3113X.2011.04588.x](https://doi.org/10.1111/j.1365-3113X.2011.04588.x) PMID: [21447069](https://pubmed.ncbi.nlm.nih.gov/21447069/)
45. Lumbreras V, Vilela B, Irar S, Sole M, Capellades M, et al. (2010) MAPK phosphatase MKP2 mediates disease responses in Arabidopsis and functionally interacts with MPK3 and MPK6. *Plant J* 63: 1017–1030. doi: [10.1111/j.1365-3113X.2010.04297.x](https://doi.org/10.1111/j.1365-3113X.2010.04297.x) PMID: [20626661](https://pubmed.ncbi.nlm.nih.gov/20626661/)
46. Vilela B, Pages M, Lumbreras V (2010) Regulation of MAPK signaling and cell death by MAPK phosphatase MKP2. *Plant Signal Behav* 5: 1497–1500. PMID: [21057191](https://pubmed.ncbi.nlm.nih.gov/21057191/)
47. Lim CW, Luan S, Lee SC (2014) A prominent role for RCAR3-mediated ABA signaling in response to *Pseudomonas syringae* pv. *tomato* DC3000 infection in Arabidopsis. *Plant Cell Physiol* 55: 1691–1703. doi: [10.1093/pcp/pcu100](https://doi.org/10.1093/pcp/pcu100) PMID: [25063782](https://pubmed.ncbi.nlm.nih.gov/25063782/)
48. Mang HG, Qian W, Zhu Y, Qian J, Kang HG, et al. (2012) Abscisic acid deficiency antagonizes high-temperature inhibition of disease resistance through enhancing nuclear accumulation of resistance proteins SNC1 and RPS4 in Arabidopsis. *Plant Cell* 24: 1271–1284. doi: [10.1105/tpc.112.096198](https://doi.org/10.1105/tpc.112.096198) PMID: [22454454](https://pubmed.ncbi.nlm.nih.gov/22454454/)
49. Mosher S, Moeder W, Nishimura N, Jikumaru Y, Joo SH, et al. (2010) The lesion-mimic mutant *cpr22* shows alterations in abscisic acid signaling and abscisic acid insensitivity in a salicylic acid-dependent manner. *Plant Physiol* 152: 1901–1913. doi: [10.1104/pp.109.152603](https://doi.org/10.1104/pp.109.152603) PMID: [20164209](https://pubmed.ncbi.nlm.nih.gov/20164209/)

50. Xu X, Chen C, Fan B, Chen Z (2006) Physical and functional interactions between pathogen-induced Arabidopsis WRKY18, WRKY40, and WRKY60 transcription factors. *Plant Cell* 18: 1310–1326. PMID: [16603654](#)
51. Swiderski MR, Birker D, Jones JD (2009) The TIR domain of TIR-NB-LRR resistance proteins is a signaling domain involved in cell death induction. *Mol Plant Microbe Interact* 22: 157–165. doi: [10.1094/MPMI-22-2-0157](#) PMID: [19132868](#)
52. Bernoux M, Ve T, Williams S, Warren C, Hatters D, et al. (2011) Structural and functional analysis of a plant resistance protein TIR domain reveals interfaces for self-association, signaling, and autoregulation. *Cell Host Microbe* 9: 200–211. doi: [10.1016/j.chom.2011.02.009](#) PMID: [21402359](#)
53. Feys BJ, Parker JE (2000) Interplay of signaling pathways in plant disease resistance. *Trends Genet* 16: 449–455. PMID: [11050331](#)
54. Caplan JL, Mamillapalli P, Burch-Smith TM, Czymmek K, Dinesh-Kumar SP (2008) Chloroplastic protein NRIP1 mediates innate immune receptor recognition of a viral effector. *Cell* 132: 449–462. doi: [10.1016/j.cell.2007.12.031](#) PMID: [18267075](#)
55. Burch-Smith TM, Dinesh-Kumar SP (2007) The functions of plant TIR domains. *Sci STKE* 2007: pe46. PMID: [17726177](#)
56. Burch-Smith TM, Schiff M, Caplan JL, Tsao J, Czymmek K, et al. (2007) A novel role for the TIR domain in association with pathogen-derived elicitors. *PLoS Biol* 5: e68. PMID: [17298188](#)
57. Shirasu K (2009) The HSP90-SGT1 chaperone complex for NLR immune sensors. *Annu Rev Plant Biol* 60: 139–164. doi: [10.1146/annurev.arplant.59.032607.092906](#) PMID: [19014346](#)
58. Azevedo C, Betsuyaku S, Peart J, Takahashi A, Noel L, et al. (2006) Role of SGT1 in resistance protein accumulation in plant immunity. *EMBO J* 25: 2007–2016. PMID: [16619029](#)
59. Bieri S, Mauch S, Shen QH, Peart J, Devoto A, et al. (2004) RAR1 positively controls steady state levels of barley MLA resistance proteins and enables sufficient MLA6 accumulation for effective resistance. *Plant Cell* 16: 3480–3495. PMID: [15548741](#)
60. Leister RT, Dahlbeck D, Day B, Li Y, Chesnokova O, et al. (2005) Molecular genetic evidence for the role of SGT1 in the intramolecular complementation of Bs2 protein activity in *Nicotiana benthamiana*. *Plant Cell* 17: 1268–1278. PMID: [15749757](#)
61. de la Fuente van Bentem S, Vossen JH, de Vries KJ, van Wees S, Tameling WI, et al. (2005) Heat shock protein 90 and its co-chaperone protein phosphatase 5 interact with distinct regions of the tomato I-2 disease resistance protein. *Plant J* 43: 284–298. PMID: [15998314](#)
62. He Y, Chung EH, Hubert DA, Tornero P, Dangl JL (2012) Specific missense alleles of the arabidopsis jasmonic acid co-receptor COI1 regulate innate immune receptor accumulation and function. *PLoS Genet* 8: e1003018. doi: [10.1371/journal.pgen.1003018](#) PMID: [23093946](#)
63. Kitagawa K, Skowrya D, Elledge SJ, Harper JW, Hieter P (1999) *SGT1* encodes an essential component of the yeast kinetochore assembly pathway and a novel subunit of the SCF ubiquitin ligase complex. *Mol Cell* 4: 21–33. PMID: [10445024](#)
64. Gray WM, Muskett PR, Chuang HW, Parker JE (2003) Arabidopsis SGT1b is required for SCF(TIR1)-mediated auxin response. *Plant Cell* 15: 1310–1319. PMID: [12782725](#)
65. Gou M, Shi Z, Zhu Y, Bao Z, Wang G, et al. (2012) The F-box protein CPR1/CPR30 negatively regulates R protein SNC1 accumulation. *Plant J* 69: 411–420. doi: [10.1111/j.1365-313X.2011.04799.x](#) PMID: [21967323](#)
66. Cheng YT, Li Y, Huang S, Huang Y, Dong X, et al. (2011) Stability of plant immune-receptor resistance proteins is controlled by SKP1-CULLIN1-F-box (SCF)-mediated protein degradation. *Proc Natl Acad Sci U S A* 108: 14694–14699. doi: [10.1073/pnas.1105685108](#) PMID: [21873230](#)
67. Consortium AIM (2011) Evidence for network evolution in an Arabidopsis interactome map. *Science* 333: 601–607. doi: [10.1126/science.1203877](#) PMID: [21798944](#)
68. Jirage D, Tootle TL, Reuber TL, Frost LN, Feys BJ, et al. (1999) Arabidopsis thaliana PAD4 encodes a lipase-like gene that is important for salicylic acid signaling. *Proc Natl Acad Sci U S A* 96: 13583–13588. PMID: [10557364](#)
69. Bowling SA, Clarke JD, Liu Y, Klessig DF, Dong X (1997) The *cpr5* mutant of Arabidopsis expresses both NPR1-dependent and NPR1-independent resistance. *Plant Cell* 9: 1573–1584. PMID: [9338960](#)
70. Thordal-Christensen H, Zhang Z, Wei Y, Collinge DB (1997) Subcellular localization of H₂O₂ in plants. H₂O₂ accumulation in papillae and hypersensitive response during the barley-powdery mildew interaction. *Plant J* 11: 1187–1194.
71. Clough SJ, Bent AF (1998) Floral dip: a simplified method for Agrobacterium-mediated transformation of *Arabidopsis thaliana*. *Plant J* 16: 735–743. PMID: [10069079](#)

72. Walter M, Chaban C, Schutze K, Batistic O, Weckermann K, et al. (2004) Visualization of protein interactions in living plant cells using bimolecular fluorescence complementation. *Plant J* 40: 428–438. PMID: [15469500](#)
73. Chen H, Zou Y, Shang Y, Lin H, Wang Y, et al. (2008) Firefly luciferase complementation imaging assay for protein-protein interactions in plants. *Plant Physiol* 146: 368–376. PMID: [18065554](#)
74. Buchner J, Grallert H, Jakob U (1998) Analysis of chaperone function using citrate synthase as nonnative substrate protein. *Methods Enzymol* 290: 323–338. PMID: [9534173](#)
75. Yoo SD, Cho YH, Sheen J (2007) Arabidopsis mesophyll protoplasts: a versatile cell system for transient gene expression analysis. *Nat Protoc* 2: 1565–1572. PMID: [17585298](#)